The Canadian Mineralogist
Vol. 42, pp. 17-42 (2004)

THE PHASE RELATIONS BETWEEN $Fe_{4.5}Ni_{4.5}S_8$ AND Co_9S_8 IN THE SYSTEM Fe–Ni–Co–S AT TEMPERATURES FROM 400° TO 1100°C

ARASHI KITAKAZE[§]

Institute of Mineralogy, Petrology and Economic Geology, Faculty of Science, Tohoku University, Aobayama, Aoba-ku, Sendai, 980-8578, Japan

ASAHIKO SUGAKI

Kadan 4-30-503, Aoba-ku, Sendai, 980-0815, Japan

ABSTRACT

Phase relations along the join $Fe_{4.5}Ni_{4.5}S_8$–Co_9S_8 in the system Fe–Ni–Co–S were investigated by the evacuated-silica-glass-tube method. Euhedral crystals of high-form cobalt pentlandite (Co_9S_8) and a member of the solid solution containing 50 mole % Co_9S_8 were also synthesized by both I_2 vapor-transport and NaCl–KCl flux methods. The phases produced in this study were examined by ore microscopy, SEM, EPMA, high-temperature X-ray diffraction and DTA. A continuous solid-solution (low form) between pentlandite and cobalt pentlandite transforms to a high-form solid-solution at temperatures from 615° ± 3°C (pentlandite) to 831° ± 3°C (cobalt pentlandite). Except for end-member compositions, there is a narrow two-phase field with both low- and high-form solid-solutions. The high–low inversion is reversible. High-form solid-solution melts incongruently to liquid and monosulfide solid-solution at temperatures from 865° ± 3°C (high-form pentlandite) to 930° ± 3°C (high-form cobalt pentlandite), and then remnant monosulfide solid-solution melts completely at temperatures from 982° ± 5°C for $(Fe,Ni)_{1-x}S$ to 1069° ± 5°C for $Co_{1-x}S$. These lines of evidence suggest that in geological processes such as the formation of Ni–Cu(–Co) ore deposits, pentlandite, Co-bearing pentlandite and Ni-bearing cobalt pentlandite can crystallize as the high form by peritectic reaction between monosulfide solid-solution segregated first from liquid (sulfide magma) and residual liquid at relatively high temperatures around 800° to 900°C. Pentlandite ($Fe_{4.5}Ni_{4.5}S_{8.0}$), cobalt pentlandite (Co_9S_8) and the member of the solid solution with 50 mole % Co_9S_8 ($Fe_{2.25}Ni_{2.25}Co_{4.50}S_{8.00}$) are cubic, $Fm\bar{3}m$, with a equal to 10.0608(2), 9.9287(2) and 9.9925(2) Å, respectively, at room temperature. On the other hand, the high forms have a primitive cubic (pc) cell with a equal to 5.335(2) Å for $Fe_{4.5}Ni_{4.5}S_{8.0}$, 5.171(2) Å for Co_9S_8, and 5.251(2) Å for the composition with 50 mole % Co_9S_8 at 850°C, corresponding to $a/2$ of the low form. The inversion of low- and high-form solid-solution is of order–disorder type, from supercell (low form) to subcell.

Keywords: pentlandite, cobalt pentlandite, solid solution, sulfide synthesis, join $Fe_{4.5}Ni_{4.5}S_8$–Co_9S_8, system Fe–Ni–Co–S, high-temperature X-ray diffraction, DTA, phase transition.

SOMMAIRE

Nous avons étudié les relations de phases du sous-système $Fe_{4.5}Ni_{4.5}S_8$–Co_9S_8 dans le système Fe–Ni–Co–S en utilisant les synthèses avec tubes de silice évacués et scellés. Nous avons aussi synthétisé des cristaux idiomorphes de la forme de haute température de cobalt pentlandite (Co_9S_8) et d'un membre de la solution solide contenant 50% de Co_9S_8 (proportion molaire), en utilisant le tranfert en phase vapeur de I_2 et un fondant NaCl–KCl. Ils ont été examinés par microcopie en lumière réfléchie, par microscopie électronique par balayage, par analyses à la microsonde électronique, par diffraction X à température élevée et par analyse thermique différentielle. Il se forme une solution solide continue de basse température entre pentlandite et cobalt pentlandite; cette structure se transforme à une forme stable à température élevée entre 615° ± 3°C (pentlandite) et 831° ± 3°C (cobalt pentlandite). Sauf pour les pôles, il y a une étroite zone de coexistence des deux phases. L'inversion est réversible. Les membres de la solution solide de haute température fondent de façon incongruente à un liquide et une solution solide monosulfurée entre 865° ± 3°C (pentlandite de haute température) et 930° ± 3°C (cobalt pentlandite de haute température), et les vestiges de la solution solide monosulfurée fondent complètement à une température entre 982° ± 5°C pour le $(Fe,Ni)_{1-x}S$ et 1069° ± 5°C pour le $Co_{1-x}S$. Ces résultats font penser que dans les contextes géologiques, par exemple lors de la formation d'un gîte minéral à Ni–Cu(–Co), pentlandite, pentlandite cobaltifère et cobalt pentlandite nickelifère peuvent cristalliser sous la forme de haute température par réaction péritectique entre la solution solide monosulfurée s'étant séparée d'abord du liquide (magma sulfuré) et le liquide résiduel à température relativement élevée, autour de 800° ou 900°C. La pentlandite ($Fe_{4.5}Ni_{4.5}S_{8.0}$), la cobalt pentlandite

§ *E-mail address*: kitakaze@cneas.tohoku.ac.jp

(Co_9S_8), et le membre de la solution solide ayant 50% de Co_9S_8 ($Fe_{2.25}Ni_{2.25}Co_{4.50}S_{8.00}$, proportion molaire) ont une symétrie cubique, $Fm\bar{3}m$, avec *a* égal à 10.0608(2), 9.9287(2) et 9.9925(2) Å, respectivement, à température ambiante. D'autre part, la structure de haute température possède une maille cubique primitive (*pc*) avec *a* égal à 5.335(2) Å pour $Fe_{4.5}Ni_{4.5}S_{8.0}$, 5.171(2) Å pour Co_9S_8, et 5.251(2) Å pour la composition contenant 50% de Co_9S_8 à 850°C, ce qui correspond à *a*/2 de la forme de basse température. L'inversion de la forme de basse température à la forme de haute température des solutions solides implique une transformation ordre–désordre en allant de la supermaille à la sous-maille.

(Traduit par la Rédaction)

Mots-clés: pentlandite, cobalt pentlandite, solution solide, synthèse de sulfures, sous-système $Fe_{4.5}Ni_{4.5}S_8$–Co_9S_8, système Fe–Ni–Co–S, diffraction X à haute température, analyse thermique différentielle, transition.

Introduction

A complete solid-solution between pentlandite, $Fe_{4.5}Ni_{4.5}S_8$, and cobalt pentlandite, Co_9S_8, forms in the system Fe–Ni–Co–S below 610°C (Knop & Ibrahim 1961, Vaasjoki *et al*. 1974, Kojonen 1976, Kaneda *et al*. 1986, Kitakaze & Sugaki 1992). The pentlandite and cobalt pentlandite end-members of the solid-solution series break down to a mixture of $Ni_{3\pm x}S_2$ and pyrrhotite (monosulfide solid-solution, *mss*), and of Co_4S_3 and $Co_{1-x}S$ (cobalt monosulfide solid-solution) at or above 610° and 833°C, respectively, according to previous studies such as those of Kullerud (1962, 1963) for pentlandite, and of Hülsmann & Weibke (1936), Rosenqvist (1954), Hansen & Anderko (1958), Kuznetsov *et al*. (1965), Vaasjoki *et al*. (1974), Rau (1976), Kojonen (1976), Lamprecht (1976, 1978), Chen & Chang (1978), and Massalski *et al*. (1990) for cobalt pentlandite.

Sugaki & Kitakaze (1992, 1998) found that pentlandite of composition $Fe_{4.5}Ni_{4.5}S_{7.9}$ does not break down at 615° ± 3°C, but rather inverts to the high form at this temperature, and it is stable up to 865° ± 3°C. They also reported that cobalt pentlandite similarly inverts to the high form at 829° ± 3°C; it has the same crystal structure as high-form pentlandite. The high form of cobalt pentlandite exists as a stable phase up to 926° ± 3°C (Kitakaze & Sugaki 1992).

The thermal stability of the solid solution between pentlandite and cobalt pentlandite was investigated by Vaasjoki *et al*. (1974) and Kojonen (1976). They reported the results of differential thermal analysis (DTA) experiments, interpreted to indicate that the solid solution breaks down at temperatures increasing from 610° to 833°C with increasing Co content. However, Kitakaze & Sugaki (1992) disagreed with this interpretation. They found that the DTA reaction reported by Vaasjoki *et al*. (1974) and Kojonen (1976) attributed to the breakdown of the solid solution actually corresponds to its inversion to the high form.

This inversion is reversible. X-ray powder-diffraction patterns at room temperature indicate that the pentlandite – cobalt pentlandite solid-solution is in the low form, which suggests that the high form is not quenchable. Therefore, it was necessary to use high-temperature X-ray diffraction, in addition to DTA, electron-probe micro-analysis (EPMA) and microscopic examination to ascertain the existence of the high form of the solid solution. New experiments involving the synthesis of pentlandite, cobalt pentlandite, the solid solution and its high form were necessary to obtain a correct phase-diagram of the $Fe_{4.5}Ni_{4.5}S_8$ – Co_9S_8 join in the quaternary system Fe–Ni–Co–S at temperatures from 400° to 1100°C. Results are described in this contribution.

The High-Temperature Syntheses

The compositions and cell-parameter data pertaining to the phases synthesized in this study are given in Table 1.

Evacuated silica-glass-tube method

Pure metals, Fe (99.999%), Ni (99.999%) and Co (99.99%), obtained from Johnson Matthey Co. Ltd., and sulfur (99.99%) from Kanto Chemical Co. Ltd., were used as starting materials for syntheses of pentlandite ($Fe_{4.5}Ni_{4.5}S_8$) and cobalt pentlandite (Co_9S_8).

For the synthesis of pentlandite, elemental Fe, Ni and S were weighed exactly in a 4.5 : 4.5 : 8.0 atomic ratio, and then sealed into a transparent silica-glass tube (inside diameter 7 mm) at 1.33×10^{-1} Pa (10^{-3} Torr). The evacuated silica-glass tube with its charge was annealed at 550°C for 10 days after heating it at 400°C for four days and at 500°C for four days. After cooling in air, the sintered charge was carefully taken out from the tube so as not to lose any of the products, ground into powder in acetone using an agate mortar, and thoroughly mixed so as to become homogeneous. The pulverized charge was sealed in an evacuated silica-glass tube again, and reheated at 550°C for 20 days. After heating, the tube was cooled in air. The resulting product, as viewed under microscope, is an aggregate of anhedral, homogeneous grains 10 to 30 μm in size.

For the synthesis of cobalt pentlandite, Co and S were precisely weighed in a 9 : 8 atomic ratio, and sealed in a silica-glass tube in the same manner as for pentlandite. The evacuated tube with its charge was annealed at 700°C for 10 days after heating at 400°C for four days. After the tube was cooled in air, the sintered charge was

carefully pulverized and mixed under acetone to produce a homogeneous mixture. The powdered charge was resealed in an evacuated silica-glass tube and reheated at 700°C for 10 days. After heating, the tube was cooled in air. The product was a microscopically homogeneous aggregate of anhedral grains 20 to 40 μm in size.

For the synthesis of members of the solid solution between pentlandite and cobalt pentlandite, we relied on a solid-state reaction between $Fe_{4.5}Ni_{4.5}S_8$ and Co_9S_8 as synthesized above. Both $Fe_{4.5}Ni_{4.5}S_8$ and Co_9S_8 were weighed exactly in accordance with the desired compositions of the solid solution at 10% intervals from 10 to 90 mole % Co_9S_8 along the $Fe_{4.5}Ni_{4.5}S_8$ – Co_9S_8 join. After grinding and thoroughly mixing under acetone to produce a homogeneous mixture, the charge was sealed in an evacuated silica-glass tube, and heated at 550°C for 20 days. The tube was cooled in air after heating. The product was an aggregate of anhedral grains 10 to 50 μm in size. The homogeneity of the products was examined by optical microscopy, X-ray powder-diffraction and EPMA. A homogeneous member of the $Fe_{4.5}Ni_{4.5}S_8$ – Co_9S_8 solid-solution was usually obtained by this method. If not, heating and grinding were repeated until the product became homogeneous.

TABLE 1. CHEMICAL COMPOSITIONS AND CRYSTALLOGRAPHIC DATA FOR MINERALS AND PHASES ENCOUNTERED IN THIS STUDY

Mineral names	Symbol	Compositions	Structure types*	References
Pentlandite	pn	$(Fe,Ni)_9S_8$ (Fe = Ni)	Cubic $Fm\bar{3}m$ *a* 10.0608(2)	Rajamani & Prewitt (1973) This study
Cobalt pentlandite	cpn	Co_9S_8	Cubic $Fm\bar{3}m$ *a* 9.9287(2)	Rajamani & Prewitt (1975a) This study
Pentlandite – cobalt pentlandite solid solution (low form)	LSS	$(Fe,Ni,Co)_9S_8$ (Fe = Ni)	Cubic $Fm\bar{3}m$ *a* 10.0608(2) – 9.9287(2)	This study
High-form pentlandite	hpn	$(Fe,Ni)_9S_8$ (Fe = Ni)	Cubic *P* *a* 5.335(2) (850°C)	Sugaki & Kitakaze (1998) This study
High-form cobalt pentlandite	hcpn	Co_9S_8	Cubic *P* *a* 5.171(2) (850°C)	This study
High-form pentlandite – cobalt pentlandite solid solution	HSS	$(Fe,Ni,Co)_9S_8$ (Fe = Ni)	Cubic *P* *a* 5.335(2) – 5.171(2) (850°C)	This study
Monosulfide solid-solution	mss	$(Fe,Ni,Co)_{1-x}S$ $Fe_{0.45}Ni_{0.48}S$	Hexagonal *P*63/*mmc* *a* 3.4343, *c* 5.5820	Misra & Fleet (1973)
High-form godlevskite	hgd	$(Ni,Fe,Co)_7S_6$ Ni_7S_6	Orthorhombic *Bmmb* *a* 3.27, *b* 16.16, *c* 11.36	Fleet (1972)
Phase β_2	β_2	$(Ni,Fe,Co)_{4+x}S_3$ Ni_4S_3	Cubic *P* *a* 5.140 (620°C)	Kitakaze & Sugaki (2001)
Heazlewoodite	hz	$(Ni,Fe,Co)_3S_2$	Hexagonal *R*32 *a* 5.747, *c* 7.135	Fleet (1977)
Phase β_1	β_1	$(Ni,Fe,Co)_{3+x}S_2$ Ni_3S_2	Cubic $Fm\bar{3}m$ *a* 5.210 (600°C)	Liné & Huber (1963) Kitakaze & Sugaki (2001)
Phase α	α	(Fe,Ni,Co) $Fe_{0.95}Ni_{0.05}$	Cubic $Im\bar{3}m$ *a* 2.8685	Raghavan (1988) Sutton & Hume-Rothery (1955)
Phase γ	γ	(Fe,Ni,Co) $Fe_{0.5}Ni_{0.5}$	Cubic $Fm\bar{3}m$ *a* 3.596	Raghavan (1988) Sumiyama *et al.* (1983)
Phase ε	ε	$(Fe,Co)(Ni,Co)_3$ $Fe_{0.26}Ni_{0.74}$	Cubic $Pm\bar{3}m$ *a* 3.5556	Raghavan (1988) Lutts & Gielen (1970)

* Cell edges in Å.

Vapor-transport method

Approximately 100 mg each of either powdered cobalt pentlandite or the member of the solid solution containing 50 mole % Co_9S_8, synthesized by the evacuated silica-tube method as above, were used as a nutrient material. The nutrient and 0.5 mg of iodine were sealed together in an evacuated tube, with an inside diameter of 5 mm and 7 cm long. The tube with its charge was kept at approximately 860°C for 20 days in a vertical electric furnace with a thermal gradient of 1.5°C/cm. Euhedral crystals (50 to 100 μm in size) of high-form cobalt pentlandite or a member of the solid solution (high form) recrystallized at approximately 850°C as a fine-grained aggregate near the top of the tube. After cooling to room temperature, the euhedral crystals were examined by optical microscopy, scanning electron microscope (SEM), and EPMA. The crystal faces were principally the well-developed (111) and (001) forms. The synthesis of pentlandite crystals by the I_2 vapor-transport method has been described by Sugaki & Kitakaze (1998).

Flux method

Approximately 200 mg of NaCl–KCl in a 1:1 molar ratio and 200 mg each of powdered cobalt pentlandite or the solid solution with 50 mole % Co_9S_8, synthesized as above, were used as starting materials. These were sealed in a silica-glass tube with an inside diameter of 5 mm and 5 cm long, under vacuum (1.33×10^{-1} Pa). The tubes with charge were kept at 850° or 800°C for 7 days, and then cooled in air. The product was recrystallized as aggregates of euhedral high-form cobalt pentlandite or solid solution, 30 to 100 μm in size. The crystal faces of this material were found to be similar to those grown by the I_2 vapor-transport method. The high form of pentlandite recrystallized by the NaCl–KCl flux method was reported by Sugaki & Kitakaze (1998).

According to EPMA analyses, the results of which are to be described below, the compositions of the single crystals of cobalt pentlandite and the solid solution synthesized by both the vapor-transport and flux methods are in good agreement with those of the nutrient or starting materials.

Experimental Procedures and Results: Microscopic Examination

Pentlandite, cobalt pentlandite, and members of the solid solution between them, synthesized at 550°, 700° and 850°C, respectively, by the evacuated silica-tube method, consist of a fine-grained aggregate of yellowish gray particles with a metallic luster at room temperature. With a reflected light microscope, synthetic pentlandite appears light creamy white in color and has a distinct octahedral cleavage. It is isotropic. The optical properties of cobalt pentlandite and members of the solid solution in polished section are the same as those of pentlandite, but their reflectance color becomes slightly more yellowish than that of pentlandite with increasing Co content. The measured values of the reflectance of synthetic pentlandite, cobalt pentlandite, and members of the solid solution between them at 10 mole % Co_9S_8 intervals for the wavelengths of 436, 497, 546, 586 and 648 nm in air and oil are presented in Table 2. The reflectance values of the solid-solution series increases continuously with increasing Co content (Fig. 1).

Under the microscope, the products along the $Fe_{4.5}Ni_{4.5}S_8$–Co_9S_8 join are mostly a single phase below temperatures of the incongruent melting (breakdown) of the solid solution. An exception is the two-phase field due to inversion of the solid solution. Also, small amounts of monosulfide solid-solution appear as granular inclusions, 10 to 30 μm in size, in pentlandite or the solid solution (0 to 35 mole % Co_9S_8), that are themselves 50–100 μm in size, as a limited field from 0 to about 35 mole % Co_9S_8 around 610° to 680°C. Similarly, small amounts of monosulfide solid-solution, which corresponds to its Co-rich end-member, that is, cobalt monosulfide $Co_{1-x}S$, occur as fine-grained inclusions in high-form cobalt pentlandite at 928° to 930°C. These are discussed below.

TABLE 2. REFLECTANCES OF SYNTHETIC PENTLANDITE, COBALT PENTLANDITE AND MEMBERS OF THE PENTLANDITE – COBALT PENTLANDITE SOLID SOLUTION IN AIR AND OIL

Compositions Mole % Co_9S_8	Wavelengths (nm) 436	497	546	586	648
		In air			
0	38.4(2)	46.0(2)	49.1(2)	51.4(2)	53.9(2)
10	39.0(2)	46.6(2)	49.6(2)	51.8(2)	54.2(2)
20	39.7(2)	47.1(2)	50.0(2)	52.0(2)	54.6(2)
30	40.2(2)	47.6(2)	50.5(2)	52.3(2)	55.0(2)
40	40.9(2)	48.1(2)	50.9(2)	52.9(2)	55.3(2)
50	41.5(2)	48.8(2)	51.4(2)	53.4(2)	55.6(2)
60	42.1(2)	49.3(2)	51.8(2)	53.8(2)	55.9(2)
70	42.7(2)	49.9(2)	52.2(2)	54.1(2)	56.2(2)
80	43.4(2)	50.4(2)	52.6(2)	54.5(2)	56.5(2)
90	43.9(2)	51.0(2)	53.2(2)	54.8(2)	56.9(2)
100	44.5(2)	51.5(2)	53.7(2)	55.2(2)	57.2(2)
		In oil			
0	36.1(2)	40.9(2)	43.6(2)	45.2(2)	47.0(2)
10	36.7(2)	41.5(2)	44.0(2)	45.6(2)	47.2(2)
20	37.4(2)	41.9(2)	44.4(2)	45.8(2)	47.6(2)
30	37.8(2)	42.4(2)	44.8(2)	46.0(2)	47.9(2)
40	38.5(2)	42.8(2)	45.2(2)	46.6(2)	48.2(2)
50	39.1(2)	43.4(2)	45.6(2)	47.0(2)	48.4(2)
60	39.6(2)	43.9(2)	46.0(2)	47.3(2)	48.7(2)
70	40.2(2)	44.4(2)	46.4(2)	47.6(2)	48.9(2)
80	40.8(2)	44.9(2)	46.7(2)	48.0(2)	49.2(2)
90	41.3(2)	45.4(2)	47.2(2)	48.2(2)	49.6(2)
100	41.9(2)	45.8(2)	47.7(2)	48.6(2)	49.8(2)

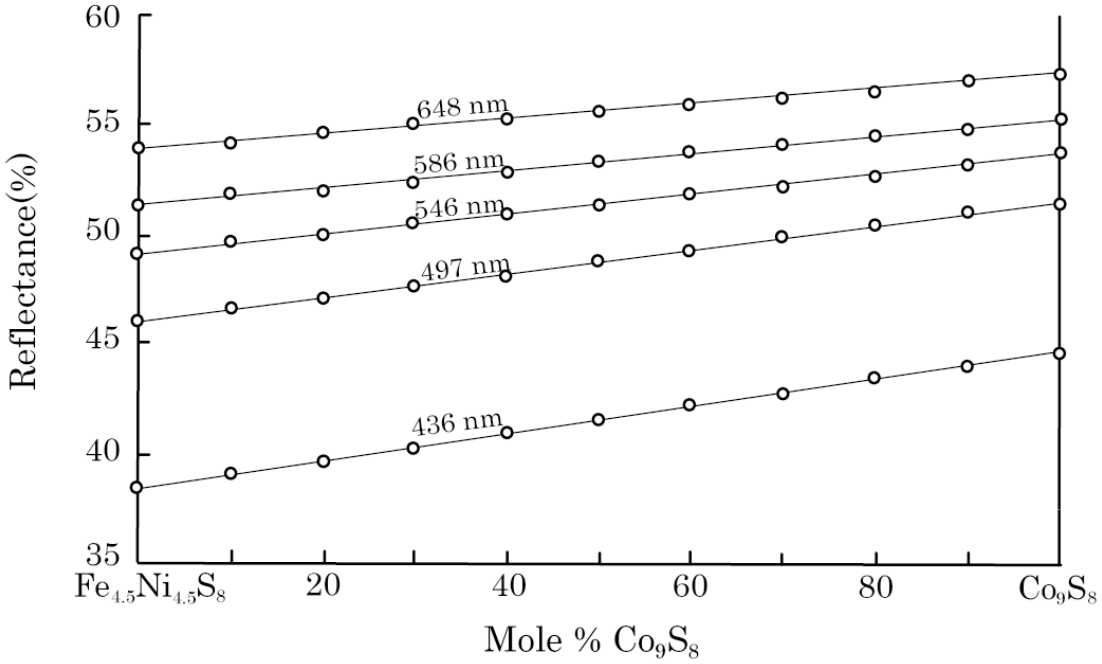

FIG. 1. The relationship between reflectance and composition for synthetic pentlandite ($Fe_{4.4}Ni_{4.5}S_8$), cobalt pentlandite (Co_9S_8) and members of the solid solution, at wavelengths of 436, 497, 546, 586 and 648 nm in air.

Monosulfide solid-solution and liquid coexist as stable phases above the temperature limits of the solid solution. After quenching, monosulfide solid-solution seems homogeneous under the microscope, but liquid invariably shows a micrographic (or eutectic) texture consisting of fine-grained crystals of pentlandite – cobalt pentlandite solid-solution, Co–Ni sulfides and alloy, less than 2 μm in size, as quench products (Fig. 2).

Fine-grained euhedral crystals obtained by both the I_2 vapor-transport and NaCl–KCl flux methods were examined by SEM. Photomicrographs of euhedral high-form cobalt pentlandite (Co_9S_8; Fig. 3A) and solid solution (50 mole % Co_9S_8; Fig. 3B) have the same morphology as pentlandite (Sugaki & Kitakaze 1998). These crystals also are homogeneous if examined by reflected light microscopy at room temperature.

ELECTRON-PROBE MICRO-ANALYSIS

The homogeneity and chemical compositions of the synthetic and equilibrium run products were examined by EPMA. Most of the products in this study consist of a single phase at equilibrium. For the evacuated silica-glass-tube experiments, the composition of the one-phase products was usually ascertained from the values of the bulk compositions of the carefully weighed starting materials. However, in order to check the accuracy of our experiments in both synthesis and equilibrium runs, the single-phase products were analyzed by EPMA (JEOL JXA–8800M).

The analytical conditions of EPMA were as follows: accelerating voltage 20 kV, specimen current measured on chalcopyrite 0.010 μA; curved crystals, LiF for Fe*K*α, Ni*K*α and Co*K*α, and TAP for S*K*α. Synthetic FeS, NiS and CoS standards were used for Fe and S, for Ni and for Co, respectively. The method of Bence & Albee (1968; Sugaki *et al.* 1976) was used to correct the X-ray intensities.

Compositional data obtained by EPMA for the pentlandite – cobalt pentlandite solid-solution as a single-phase product obtained by synthesis and equilibrium runs are given in Table 3, together with the bulk compositions of the starting materials in the evacuated-silica-tube method. The compositions are in good agreement.

Euhedral crystals of the high-form cobalt pentlandite and the solid solution with 50 mole % Co_9S_8 recrystallized by the I_2 vapor-transport and NaCl–KCl flux methods seem homogeneous. They have the following compositions, determined by EPMA: $Co_{9.01}S_{7.99}$ at 850°C (vapor transport) and $Co_{8.99}S_{8.01}$ at 850°C (flux) for high-form cobalt pentlandite, and $Fe_{2.23}Ni_{2.21}Co_{4.55}S_{8.01}$ at 850°C (vapor transport) and $Fe_{2.24}Ni_{2.24}Co_{4.51}S_{8.01}$ at 800°C (flux) for the midpoint of the solid solu-

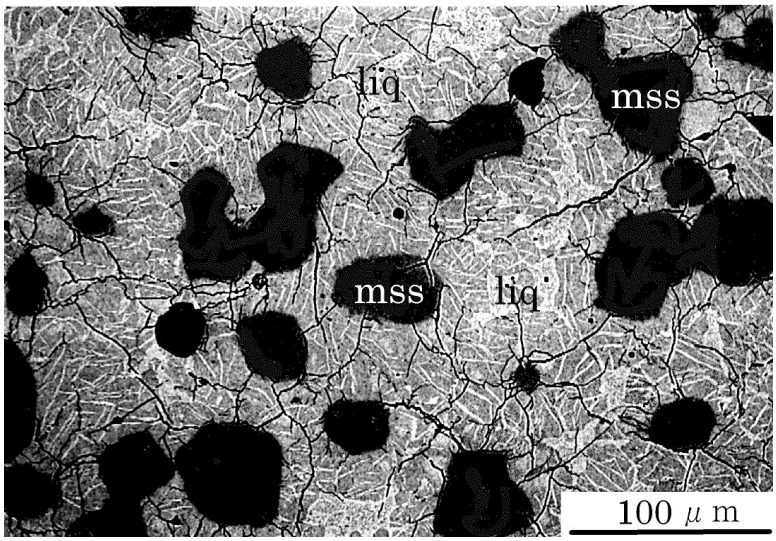

FIG. 2. Back-scattered electron image by EPMA of coexisting monosulfide solid-solution (mss) and liquid (liq) for a 60 mole % Co_9S_8 bulk composition at 950°C. Liquid is a mixture of pentlandite – cobalt pentlandite solid-solution (gray) and alloy (light gray) as quenched products.

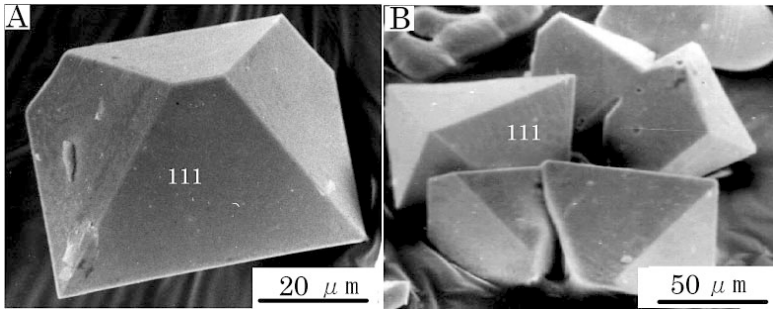

FIG. 3. SEM photomicrographs of high-form cobalt pentlandite and solid-solution crystals. A. Euhedral crystal of high-form cobalt pentlandite ($Co_{9.01}S_{7.99}$) synthesized by the I_2 vapor-transport method at 850°C. B. aggregate of euhedral crystals of high-form pentlandite – cobalt pentlandite solid-solution ($Fe_{2.24}Ni_{2.24}Co_{4.51}S_{8.01}$) synthesized by the NaCl – KCl flux method at 800°C.

tion (Table 4). These compositions of cobalt pentlandite and the solid solution that recrystallized as the high form exactly match those used for nutrient or as starting materials, Co_9S_8 and $Fe_{2.25}Ni_{2.25}Co_{4.50}S_{8.00}$ (50 mole % Co_9S_8). On the other hand, EPMA data for euhedral crystals of Co-free high-form pentlandite give $Fe_{3.06–3.87}Ni_{5.13–5.91}S_{7.19–7.70}$ at 770°C (vapor transport) and $Fe_{4.25–5.03}Ni_{3.97–4.75}S_{7.89–8.08}$ at 800°C (flux) (Sugaki & Kitakaze 1998).

Monosulfide solid-solution and liquid coexist as a breakdown product of the continuous solid-solution (high form) along the $Fe_{4.5}Ni_{4.5}S_8$ – Co_9S_8 binary join at temperatures higher than the incongruent melting of the solid solution. However, the pair monosulfide solid-solution + liquid coexisting in an equilibrium state have compositions that are off the $Fe_{4.5}Ni_{4.5}S_8$ – Co_9S_8 join, indicating that the join is pseudobinary. It was necessary to use electron-microprobe data to determine their

TABLE 3. CHEMICAL COMPOSITIONS OF PENTLANDITE – COBALT PENTLANDITE SOLID-SOLUTION SERIES SYNTHESIZED BY THE EVACUATED SILICA-GLASS TUBE METHOD AT 500°C, AS OBTAINED BY ELECTRON-PROBE MICRO-ANALYSIS

	Starting compositions				EPMA data								
Mole %	Weight %				Weight %					Atomic %			
Co_9S_8	Fe	Ni	Co	S	Fe	Ni	Co	S	Total	Fe	Ni	Co	S
0	32.55	34.22	0.00	33.23	32.6	34.2	0.0	33.3	100.1	26.5	26.4	0.0	47.1
10	29.24	30.74	6.86	33.16	29.3	30.7	6.7	33.1	99.8	23.9	23.8	5.2	47.1
20	25.94	27.27	13.69	33.10	25.8	27.3	13.7	33.1	99.9	21.1	21.2	10.6	47.1
30	22.66	23.82	20.49	33.03	22.8	23.7	20.3	33.0	99.8	18.7	18.5	15.8	47.0
40	19.38	20.38	27.27	32.97	19.4	20.2	27.4	32.9	99.9	15.9	15.8	21.3	47.0
50	16.12	16.95	34.02	32.91	16.1	16.9	34.0	32.9	99.9	13.2	13.2	26.5	47.1
60	12.87	13.53	40.75	32.85	12.7	13.7	40.9	32.8	100.1	10.4	10.7	31.9	47.0
70	9.64	10.13	47.45	32.78	9.7	10.2	47.4	32.7	100.0	8.0	8.0	37.0	47.0
80	6.41	6.74	54.13	32.72	6.4	6.7	54.1	32.6	99.8	5.3	5.3	42.4	47.0
90	3.20	3.36	60.78	32.66	3.2	3.3	61.0	32.6	100.1	2.6	2.6	47.8	47.0
100	0.00	0.00	67.40	32.60	0.0	0.0	67.4	32.7	100.1	0.0	0.0	52.9	47.1

TABLE 4. EPMA DATA FOR EUHEDRAL CRYSTALS OF HIGH-FORM COBALT PENTLANDITE AND THE MIDPOINT OF THE SOLID SOLUTION, SYNTHESIZED BY I_2 VAPOR-TRANSPORT AND NaCl–KCl FLUX METHODS

Methods	SC	T	Weight %					Atomic %			
		°C	Fe	Ni	Co	S	Total	Fe	Ni	Co	S
Vapor transport	50	850	16.0	16.8	34.6	33.1	100.5	13.1	13.0	26.8	47.1[1]
	100	850	0.0	0.0	67.7	32.7	100.4	0.0	0.0	53.0	47.0[2]
Flux	50	800	16.1	17.0	34.2	33.1	100.4	13.2	13.2	26.5	47.1[3]
	100	850	0.0	0.0	67.6	32.8	100.4	0.0	0.0	52.9	47.1[4]

SC: starting composition, expressed in mole % Co_9S_8.
1) $Fe_{2.23}Ni_{2.21}Co_{4.55}S_{8.01}$, 2) $Co_{9.01}S_{7.99}$, 3) $Fe_{2.24}Ni_{2.24}Co_{4.51}S_{8.01}$, 4) $Co_{8.99}S_{8.01}$.

TABLE 5. CHEMICAL COMPOSITIONS OBTAINED BY EPMA FOR COEXISTING MONOSULFIDE SOLID-SOLUTION AND LIQUID IN THE TWO-PHASE FIELD ALONG THE $Fe_{4.5}Ni_{4.5}S_8$ – Co_9S_8 JOIN AT 950°C

SC	Phase	Weight %					Atomic %			
mole % Co_9S_8		Fe	Ni	Co	S	Total	Fe	Ni	Co	S
0.0	mss	34.9	28.7	0.0	36.4	100.0	27.8	21.7	0.0	50.5
	liq	25.0	42.4	0.0	32.6	100.0	20.5	33.0	0.0	46.5
10.0	mss	36.0	27.3	0.1	36.4	99.8	28.7	20.7	0.1	50.5
	liq	19.6	33.3	15.1	32.1	100.1	16.1	26.1	11.8	46.0
20.0	mss	37.7	25.4	0.1	36.3	99.5	30.1	19.3	0.1	50.5
	liq	15.1	27.9	25.2	31.8	100.0	12.5	21.9	19.8	45.8
30.0	mss	39.6	24.0	0.1	36.5	100.2	31.4	18.1	0.1	50.4
	liq	11.6	24.0	32.8	31.5	99.9	9.6	19.0	25.8	45.6
40.0	mss	41.1	22.2	0.1	36.3	99.7	32.7	16.8	0.1	50.4
	liq	7.8	19.5	41.7	31.1	100.1	6.5	15.5	32.9	45.1
50.0	mss	40.8	18.9	4.0	36.3	100.0	32.4	14.3	3.0	50.3
	liq	6.2	16.8	46.4	30.7	100.1	5.2	13.4	36.7	44.7
60.0	mss	33.9	13.3	17.0	35.8	100.0	27.1	10.1	12.9	49.9
	liq	4.0	13.9	51.4	30.4	99.7	3.4	11.1	41.0	44.5
70.0	mss	23.3	7.3	33.7	35.8	100.1	18.7	5.6	25.6	50.1
	liq	3.2	11.3	54.9	30.3	99.7	2.7	9.1	43.8	44.4
80.0	mss	16.1	3.9	44.3	35.7	100.0	13.0	3.0	33.8	50.2
	liq	1.3	9.0	59.9	30.1	100.3	1.1	7.2	47.7	44.0
90.0	mss	8.0	1.3	55.1	35.4	99.8	6.5	1.0	42.4	50.1
	liq	0.8	5.0	64.0	30.0	99.8	0.7	4.0	51.2	44.1
100.0	mss	0.0	0.0	64.9	35.3	100.2	0.0	0.0	50.0	50.0
	liq	0.0	0.0	70.1	30.0	100.1	0.0	0.0	56.0	44.0

Symbols: mss: monosulfide solid-solution, liq: liquid. SC: starting composition.

compositions. Because the quenched liquid usually contains a lot of fine-grained quench products (Fig. 2), a 5-μm electron beam was scanned over an area of 40 to 50 μm square so as to cover a sufficiently large area in order to determine the original compositions of liquid before quenching. The EPMA data for a pair of monosulfide solid-solution + liquid at 950°C are given in Table 5. Monosulfide solid-solution produced by the breakdown (incongruent melting) of the solid solution in the composition range from 10 to 40 mole % Co_9S_8 contains only 0.1 at.% Co regardless of the fact that the original solid-solution contains from 5.29 (10 mole % Co_9S_8) to 21.18 at.% Co (40 mole % Co_9S_8). However, the Co content of monosulfide solid-solution produced from the original solid-solution containing more than 50 mole % Co_9S_8 increases rapidly, although it is invariably less than that of the solid solution. Also, the Fe content of monosulfide solid-solution increases with increasing Co content of the original solid-solution (0 to 50 mole % Co_9S_8), but decreases for the solid solution containing more than 60 mole % Co_9S_8. The liquid invariably becomes more Co-rich than the original solid-solution. The monosulfide solid-solution is invariably more S-rich than the original solid-solution; conversely, the liquid is more S-poor.

High-Temperature X-Ray Diffraction

X-ray powder-diffraction up to 700°C

As mentioned above, the high form on the join $Fe_{4.5}Ni_{4.5}S_8 - Co_9S_8$ is not quenchable. The phase was characterized using an X-ray powder diffractometer (JEOL JDX–7S) with a high-temperature unit (JEOL DX–GOHV2) operable to 700°C, as described by Sugaki & Kitakaze (1998). The surface of the sample was coated with a film of gold in a vacuum evaporator to keep it flat up to 700°C and to prevent oxidation. The heating unit was evacuated, and then filled up with a purified nitrogen gas. The X-ray powder patterns were taken using Cu*K*α radiation (35 kV, 15 mA) in a slow flow of nitrogen gas after keeping the sample at the desired temperature for a hour. The gold coating was also used as an internal standard to correct for the reflection peaks in the powder pattern at high temperature by making use of its well-established coefficient of expansion. Metallic silicon also was used as an internal standard, but it tends to react with the sample at a high temperature. Temperature was measured with a Pt–Pt•Rh(13%) thermocouple inserted into a small well in the sample holder. The temperature difference between the well and sample was within ±2° at 600°C. The temperature during the measurements was regulated to within ±1°C.

X-ray powder diffraction from 700° to 930°C

The powder-diffraction patterns for the members of the solid solution along the $Fe_{4.5}Ni_{4.5}S_8 - Co_9S_8$ join, including both the end members, were recorded at high temperatures above 700° up to 930°C using an imaging plate (IP) X-ray diffractometer (Rigaku R–AXIS IV^{++}) with a high-temperature unit. This apparatus has an X-ray generator with a rotating anode as a source.

A small amount (~0.5 mg) of the powder sample was put into the bottom of a silica-glass capillary tube, 0.5 mm in diameter and about 3 cm long, which had been drawn into a capillary from an ordinary transparent silica-glass tube, 5 mm in diameter. The narrow end of the capillary was sealed in a high-temperature flame. The other end of the capillary remained connected to the original tube from which it had been drawn. After inserting the sample as above, a silica-glass fiber was inserted into the capillary to prevent the sample from moving. The capillary was then evacuated together with the original tube connected to a rotary vacuum pump, and sealed. The silica-glass fiber stopped the sample powder from being sucked out when the capillary was being evacuated. The sealed capillary was placed in the X-ray diffractometer so as to keep the sample at the top of the capillary and was then covered with an electric furnace wound with a Pt wire.

After keeping the capillary at the desired temperature for a hour, the sample was examined by the X-ray diffraction using Cu*K*α radiation (50 kV, 100 mA) for 15 minutes at the same temperature. The X-ray reflections for the sample were recorded on the imaging plate (IP). The position and intensity of the reflections were examined by scanning with laser light in the IP reading system. Treating these data by computer resulted in an X-ray powder pattern being obtained for the sample more speedily than the previous method using a moving high-temperature Debye–Scherrer cassette camera.

Temperature was measured with a Pt–Pt•Rh(13%) thermocouple set 1 mm from the sample capillary and controlled continuously by a regulator to within ±1°C during the experiment. The temperature difference between the head of the thermocouple and sample was within ±5° at 850°C.

The results of the powder-diffraction investigation

According to Sugaki & Kitakaze (1998), the high-temperature X-ray powder pattern of pentlandite of composition $Fe_{4.5}Ni_{4.5}S_{7.8}$ differs markedly above 620°C from that of the same sample below 580°C. The same can be expected for cobalt pentlandite and members of the solid solution. Powder patterns of the solid solution containing 0 to 100 mole % Co_9S_8 at intervals of 10 mole % were taken at temperatures from room temperature to 930°C. As examples, the powder patterns of cobalt pentlandite and the solid solution with 50 mole % Co_9S_8 ($Fe_{2.25}Ni_{2.25}Co_{4.50}S_8$) at room temperature, 400°, 600° and 850°C and at room temperature, 400°, 725° and 850°C, respectively, are shown in Figures 4 and 5.

The powder pattern of Co_9S_8 at 850°C differs from that at 600°C and below (Fig. 4). The reflections of type $h + k + l \neq 2n$ (hereafter $hkl \neq 2n$) are present below 800°C, but disappear at 850°C, whereas the reflections of type $hkl = 2n$, except for those of 200 and 400, remain. We believe that this change in the reflections is due to the inversion to the high form of cobalt pentlandite, as in the case of high-form pentlandite (Sugaki & Kitakaze 1998). The same change as the inversion of cobalt pentlandite is also seen in the powder patterns of the solid solution containing 50 mole % Co_9S_8 at 400° and 800°C, indicating the presence of the low and high forms, respectively (Fig. 5). However, the powder pattern at 725°C is complicated by the presence of the reflections belonging to both the low and high forms of the solid solution.

The values of the unit-cell edge a and of d_{311} and d_{222} *versus* temperature for cobalt pentlandite and the solid solution containing 50 mole % Co_9S_8 increase linearly with increasing temperature (Figs. 6, 7) in a manner similar to those of pentlandite (Sugaki & Kitakaze 1998). Figure 7 shows a limited two-phase field of coexisting low- and high-form solid-solution in the temperature range from 695° to 733°C (DTA data, presented below).

X-ray powder-diffraction data for synthetic cobalt pentlandite and the member of the solid solution containing 50 mole % Co_9S_8 at room temperature, 400° and 600°C, and their high forms at 850°C, are given in Tables 6 and 7, respectively. The reflections of the high form of both compounds were indexed in terms of a cubic cell with *a*/2 of cobalt pentlandite and the low form of the solid solution because all the reflections for the high form of cobalt pentlandite and the solid solution at 850°C correspond to those of type $hkl = 2n$ for their low form. The powder-diffraction data (Tables 6, 7) of cobalt pentlandite and the low form of the solid solution indicate that they belong to space group $Fm\bar{3}m$, as previously determined by Lindqvist *et al*. (1936), Geller (1962), and Rajamani & Prewitt (1975a). The unit cell of their high form is a primitive cubic (*pc*) lattice similar to high-form pentlandite (Sugaki & Kitakaze 1998); the change is reversible. At 850°C, no reflections indicative of the appearance of other phases, for instance monosulfide solid-solution, were found.

TABLE 6. X-RAY POWDER-DIFFRACTION DATA FOR SYNTHETIC COBALT PENTLANDITE (Co_9S_8) AT ROOM TEMPERATURE, 400° AND 600°C, AND FOR ITS HIGH FORM AT 850°C

Cobalt pentlandite							High-form cobalt pentlandite 850°C		
Room temperature			400°C		600°C				
hkl	I	*d*(obs.)	I	*d*(obs.)	I	*d*(obs.)	*hkl*	I	*d*(obs.)
111	30	5.7324	25	5.852	23	5.909			
200	6	4.9645	5	5.069	4	5.114			
220	6	3.5103	5	3.582	4	3.619	110	5	3.657
311	100	2.9937	100	3.056	100	3.086			
222	30	2.8662	40	2.927	50	2.953	111	20	2.985
400	5	2.4821	5	2.534	5	2.557			
331	15	2.2779	13	2.326	10	2.348			
420	3	2.2201	3	2.265	3	2.287			
422	2	2.0268	1	2.070	1	2.088			
511	35	1.9109	20	1.950	17	1.970			
440	100	1.7553	80	1.791	70	1.809	220	100	1.829
531	4	1.6783	3	1.714	3	1.731			
600	1	1.6549	1	1.690	1	1.706			
620	1	1.5700	1	1.603	1	1.618			
533	9	1.5142	10	1.545	10	1.560			
622	9	1.4970	10	1.528	10	1.543	311	8	1.559
444	1	1.4332	1	1.463	1	1.477	222	4	1.493
551	2	1.3902	2	1.420	1	1.433			
a (Å)		9.9287(2)		10.135(2)		10.232(2)			5.171(2)

Single-crystal X-ray diffraction

X-ray-diffraction patterns for single crystals of cobalt pentlandite of composition $Co_{9.01}S_{7.99}$ and

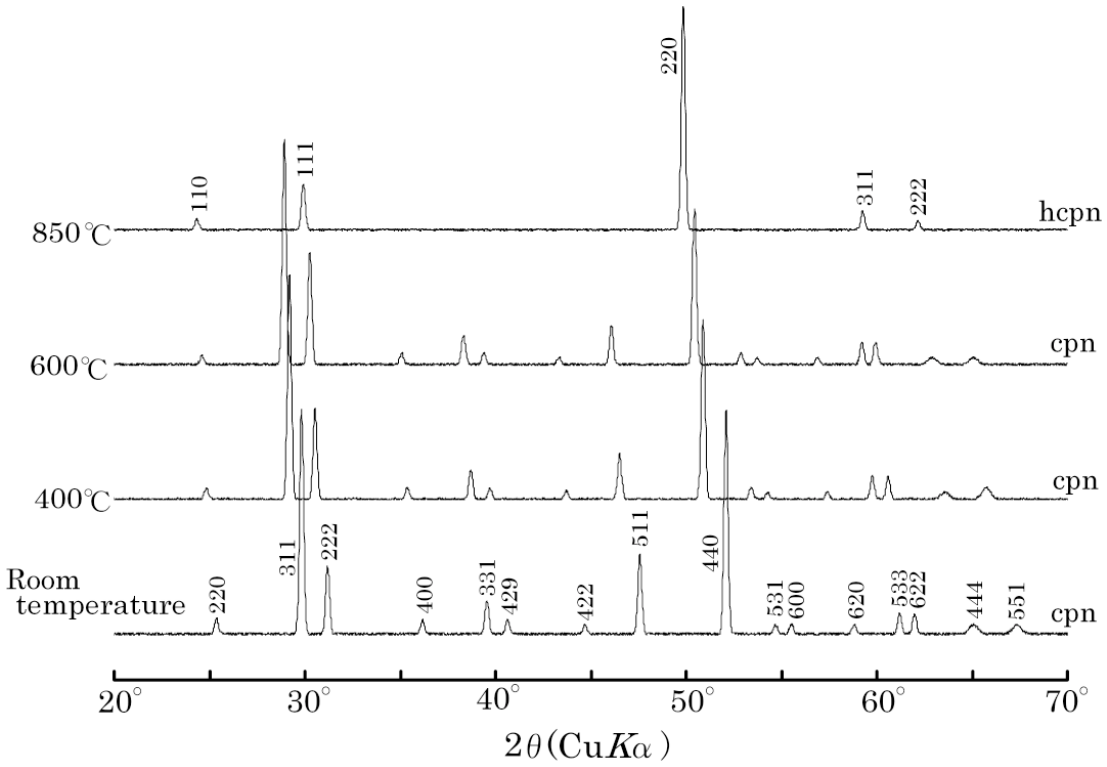

FIG. 4. X-ray powder-diffraction patterns of synthetic cobalt pentlandite and its high form (Co_9S_8) at room temperature, 400° and 600° and at 850°C, respectively. See Table 1 for symbols.

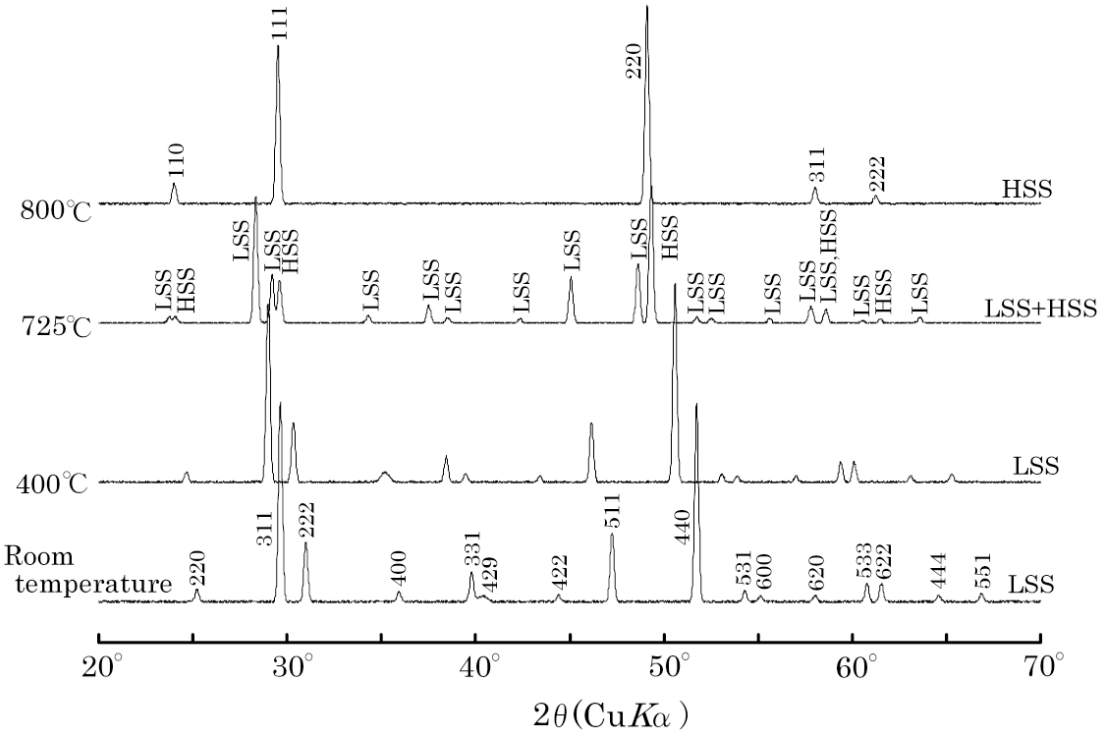

FIG. 5. X-ray powder-diffraction patterns for synthetic low- and high-form members of the solid solution with 50 mole % Co_9S_8 at room temperature, 400° and 800°C, respectively. The pattern at 725°C shows reflections for coexisting low and high forms. See Table 1 for symbols.

TABLE 7. X-RAY POWDER-DIFFRACTION DATA FOR PENTLANDITE – COBALT PENTLANDITE SS (50 MOLE % Co_9S_8) AT ROOM TEMPERATURE, 400° AND 600°C, AND FOR ITS HIGH FORM AT 850°C

Pentlandite – cobalt pentlandite solid solution, 50 mole % Co_9S_8							High-form solid solution		
Room temperature			400°C		600°C		850°C		
hkl	I	*d*(obs.)	I	*d*(obs.)	I	*d*(obs.)	*hkl*	I	*d*(obs.)
111	30	5.7693	25	5.906	23	5.970			
200	6	4.9962	5	5.113	4	5.168			
220	6	3.5330	5	3.616	4	3.655	110	10	3.713
311	100	3.0130	90	3.083	90	3.118			
222	30	2.8846	30	2.954	30	2.984	111	80	3.032
400	5	2.4982	5	2.558	5	2.585			
331	15	2.2924	13	2.346	13	2.373			
420	3	2.2346	3	2.286	3	2.311			
422	2	2.0395	1	2.087	1	2.110			
511	35	1.9231	30	1.969	33	1.991			
440	100	1.7665	100	1.809	100	1.827	220	100	1.856
531	4	1.6891	3	1.728	3	1.747			
600	1	1.6654	1	1.704	1	1.724			
620	1	1.5891	1	1.615	1	1.636			
533	9	1.5237	10	1.558	10	1.576			
622	9	1.5064	10	1.539	10	1.560	311	8	1.582
444	1	1.4424	1	1.477	1	1.492	222	4	1.516
551	2	1.3992	2	1.431	1	1.448			
a (Å)		9.9925(2)		10.227(2)		10.339(2)			5.255(2)

$Co_{8.99}S_{8.01}$ synthesized by the vapor-transport and flux methods, respectively, at 850°C and of the solid solution of composition $Fe_{2.23}Ni_{2.21}Co_{4.55}S_{8.01}$ and $Fe_{2.24}Ni_{2.24}Co_{4.51}S_{8.01}$ (~50 mole % Co_9S_8) synthesized at 850° (vapor transport) and 800°C (flux), respectively (Table 4), were prepared at room temperature, 600° and 850°C using the IP X-ray diffractometer. The single crystal was placed in the bottom of a 0.5-mm-diameter silica-glass capillary closed at the end and held in place by a silica-glass fiber inserted into the capillary, similar to the case for the powder sample. The tube was evacuated and sealed. After setting it on the diffractometer, the crystal was equilibrated at the desired temperature for an hour. Exposure to Cu*K*α radiation (50 kV, 100 mA) was then made for a hour, oscillating the single crystal ±15° at the same temperature. The position and intensity of the reflection spots for the single crystal were recorded on the IP, and the diffraction data and unit-cell edge for the single crystal were obtained in a manner similar to the powder-diffraction data above 700°C.

The diffraction spots of [110] oscillation images on the IP at room temperature and 600°C for a single crys-

tal of cobalt pentlandite of composition $Co_{9.01}S_{7.99}$, synthesized by the vapor-transport method at 850°C, were 111, 002, 220, 113, 222, 004, 331 and 440, belonging to both $hkl \neq 2n$ and $hkl = 2n$, as shown in Figure 8A. From these diffraction data, the values of the edge of the cubic cell were calculated to be 9.927(5) and 10.231(5) Å at room temperature and 600°C, respectively. However, diffraction spots observed at 850°C were only those corresponding to the type $hkl = 2n$ reflections at room temperature and 600°C; those of type $hkl \neq 2n$ reflections had disappeared (Fig. 8A). The reflections remaining at 850°C were indexed as 110, 111 and 220 for the cubic cell with a cell edge half that of cobalt pentlandite (low form), similar to those obtained by powder diffraction. The unit-cell edge a of the single crystal ($Co_{9.01}S_{7.99}$) is 5.165(5) Å. An X-ray-diffraction pattern of a single crystal of cobalt pentlandite of composition $Co_{8.99}S_{8.01}$ synthesized at 850°C by the flux method was also determined at room temperature, 600° and 850°C. These results are in good agreement with those for the crystal of composition $Co_{9.01}S_{7.99}$ (vapor transport) mentioned above.

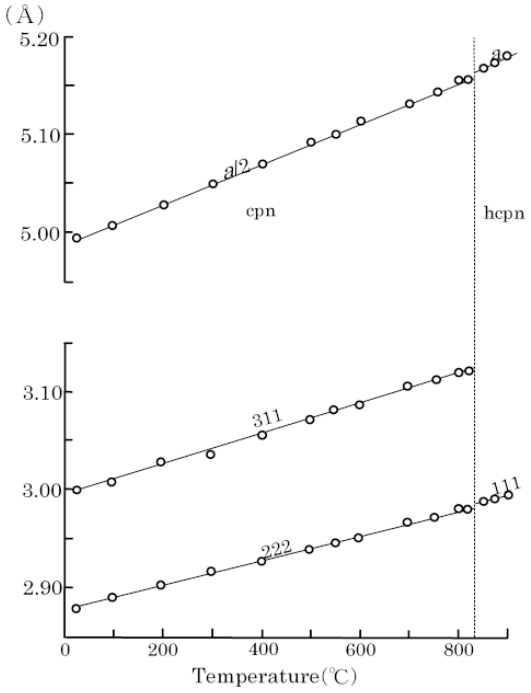

FIG. 6. The unit-cell edge and values of d_{311} and d_{222} of cobalt pentlandite (Co_9S_8) and d_{111} of its high form *versus* temperature. The dashed line at 831°C indicates the boundary between the two phases (high–low inversion). See Table 1 for symbols.

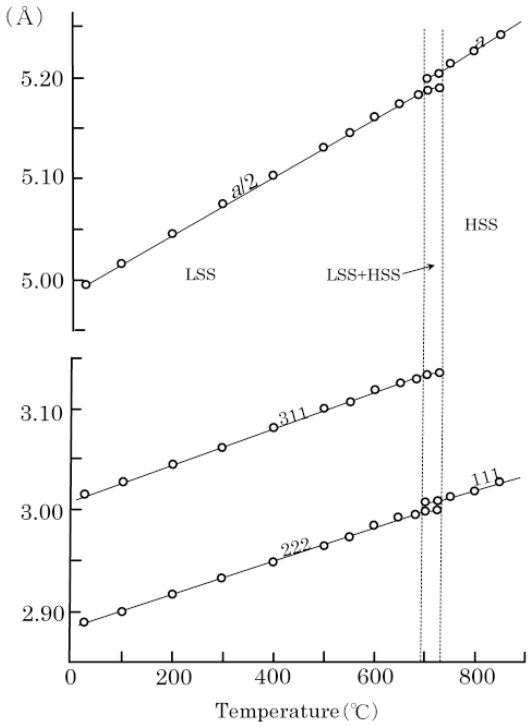

FIG. 7. The unit-cell edge and values of d_{311} and d_{222} of pentlandite – cobalt pentlandite solid-solution with 50 mole % Co_9S_8 and d_{111} of its high form *versus* temperature. A two-phase field of the low and high forms lies between 695° and 733°C. See Table 1 for symbols.

We also examined a single crystal of composition $Fe_{2.23}Ni_{2.21}Co_{4.55}S_{8.01}$, synthesized by the vapor-transport method at 850°C, by X-ray diffraction at room temperature, 600° and 850°C. The diffraction patterns are shown in Figure 8B. These patterns are almost the same as those of cobalt pentlandite and its high form (Fig. 8A), although the spacings and intensities of the reflections differ somewhat. The values of the unit-cell edge a are 9.991(5), 10.335(5) and 5.252(5) Å at room temperature, 600° and 850°C, respectively. Another single crystal of composition $Fe_{2.24}Ni_{2.24}Co_{4.51}S_{8.01}$, synthesized by the flux method at 800°C was examined by X-ray diffraction at the same temperatures. The results conform entirely to those above.

From the results of the high-temperature X-ray powder-diffraction and single-crystal diffraction, it is clear that a reversible phase-transition occurs with an attendant change in the size of the unit cell. The unit-cell edge doubles at 831° ± 3°C (DTA data) for cobalt pentlandite, and over a temperature range from 733° ± 3°C to 695° ± 3°C (DTA) for the composition with 50 mole % Co_9S_8. No compositional change was found at the

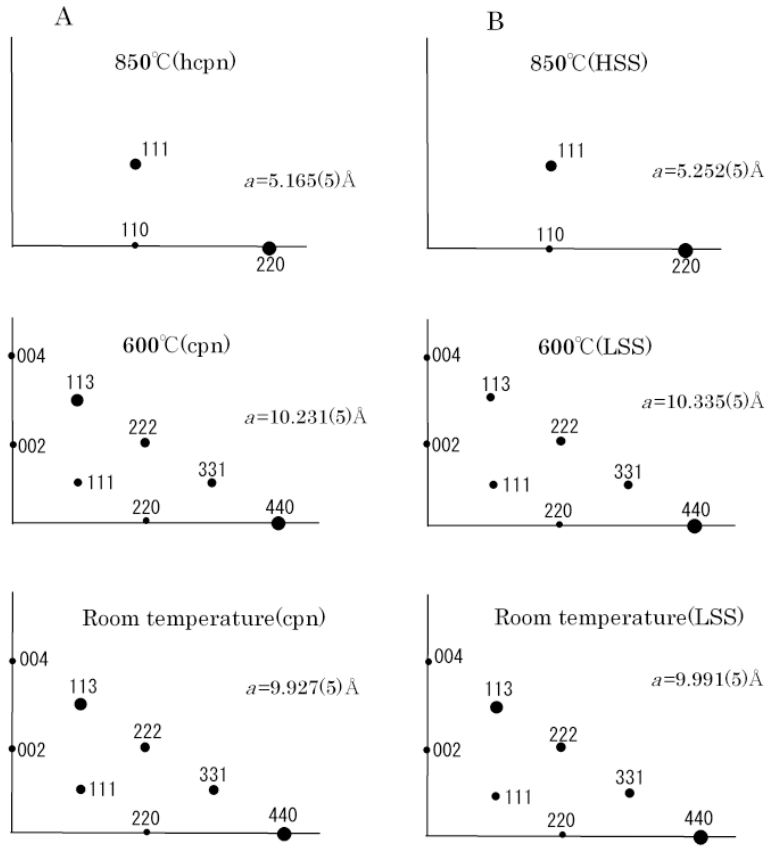

FIG. 8. [110] oscillation images obtained by single-crystal X-ray diffraction with an IP X-ray diffractometer, for a euhedral crystal of cobalt pentlandite and a member of the solid solution at room temperature and 600°C, and their high form at 850°C, respectively. A. Cobalt pentlandite of composition $Co_{9.01}S_{7.99}$, B. Solid solution of the composition $Co_{4.55}Fe_{2.23}Ni_{2.21}S_{8.01}$. Both the crystals were synthesized by the I_2 vapor-transport method at 850°C. See Table 1 for symbols.

transition. It is possible that this transition is an order–disorder inversion from the supercell (low form) to the subcell, similar to that encountered in pentlandite (Sugaki & Kitakaze 1998).

DIFFERENTIAL THERMAL ANALYSIS

We carried out differential thermal analyses to ascertain the thermal behavior and stability of the solid solution prepared at intervals of 10 mole % Co_9S_8 along the join $Fe_{4.5}Ni_{4.5}S_8$ – Co_9S_8, including the end members. The samples were synthesized at 500°C by the evacuated silica-tube method. For each experiment, 300 mg of powdered sample was sealed in an evacuated tube with an inside diameter of 5 mm. Alpha-alumina sealed in the evacuated tube was used as a reference material. The bottom of the sealed tubes was prepared with a hole for inserting the thermocouples. Chromel–alumel thermocouples sheathed with Inconel were used for both the differential and sample temperatures.

The DTA was normally performed at fixed heating rates of 5°C/min from room temperature to 1100°C. In some cases, a slow rate of heating, 1° or 2°C/min, was used from 550° to 1100°C, in order to pinpoint more accurately the temperatures of the thermal reactions. The temperature was calibrated using the melting or freezing points of high-purity Sn (231.97°C), Zn (419.6°C), Al (660.40°C), Ag (961.9°C) and Au (1064.43°C).

As shown in Figure 9, there are two strong endothermic reactions, labeled T_1–T_2 and T_3. The temperatures of the reaction increase with increasing Co content. A first reaction at 615° and 831° ± 3°C for $Fe_{4.5}Ni_{4.5}S_8$

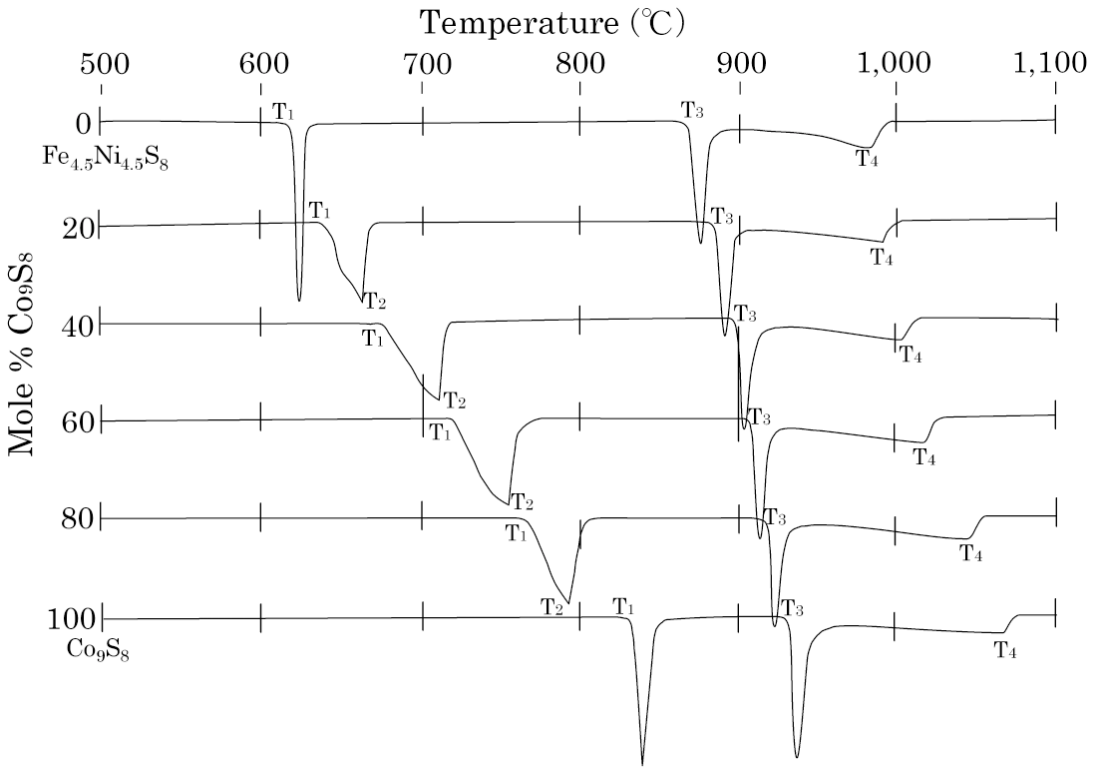

FIG. 9. DTA curves for the $Fe_{4.5}Ni_{4.5}S_8$ – Co_9S_8 solid-solution containing 0, 20, 40, 60, 80 and 100 mole % Co_9S_8. The values for T_1, T_2, T_3 and T_4 are given in Table 8.

TABLE 8. TEMPERATURES OF REACTION IN MEMBERS OF THE $Fe_{4.5}Ni_{4.5}S_8$ – Co_9S_8 SOLID SOLUTION SYNTHESIZED AT 500°C, AS OBTAINED BY DIFFERENTIAL THERMAL ANALYSIS

Mole % Co_9S_8	Reaction temperatures (°C)			
	T1	T2	T3	T4
0.00	615	–	865	982
11.11	625	642	875	986
20.00	637	663	883	990
30.00	655	687	889	997
40.00	675	710	895	1003
50.00	695	733	900	1010
60.00	718	753	905	1020
70.00	743	773	910	1033
80.00	765	792	915	1045
90.00	792	813	920	1055
100.00	831	–	930	1069

T1: High–low inversion, T2: end of the inversion, T3: breakdown (inconguent melting) of high form, T4: complete melting.

and Co_9S_8, respectively, appears as a sharp single peak in the curves. However, the curves of this reaction for the solid-solution compositions from 20 to 80 mole % Co_9S_8 show a broad peak with a shoulder continued from T_1 to T_2. The T_1–T_2 range is from 17 to 38°C. A second strong reaction (T_3) appears as a steep peak, but still continues as a gentle endothermic reaction with increasing temperature, and terminates at temperatures (T_4) ranging from 982° ± 5°C ($Fe_{4.5}Ni_{4.5}S_8$) to 1069° ± 5°C (Co_9S_8) with increasing Co content. The reaction temperatures ($T_{1–4}$) for the compositions of the solid solution are given in Table 8. These reactions are reversible. When a sample heated above 1100°C was cooled at the spontaneous cooling-rate (~5°C/min) in the same furnace, these same reactions appeared as exothermic peaks in the DTA curve. For instance, the endothermic reactions in the heating curve for cobalt pentlandite are clearly seen as exothermic peaks in the cooling curve (Fig. 10), similar to those for Co-free pentlandite (Sugaki & Kitakaze 1998).

After considering all the data, derived by observations under the microscope, EPMA, X-ray diffraction and DTA, we conclude that the feature extending with increasing Co content from 615° ± 3°C ($Fe_{4.5}Ni_{4.5}S_{8.0}$) to 831° ± 3°C (Co_9S_8) is a high–low inversion, and the feature extending from 865° ± 3°C ($Fe_{4.5}Ni_{4.5}S_{8.0}$) to 930° ± 3°C (Co_9S_8) is the breakdown (incongruent melt-

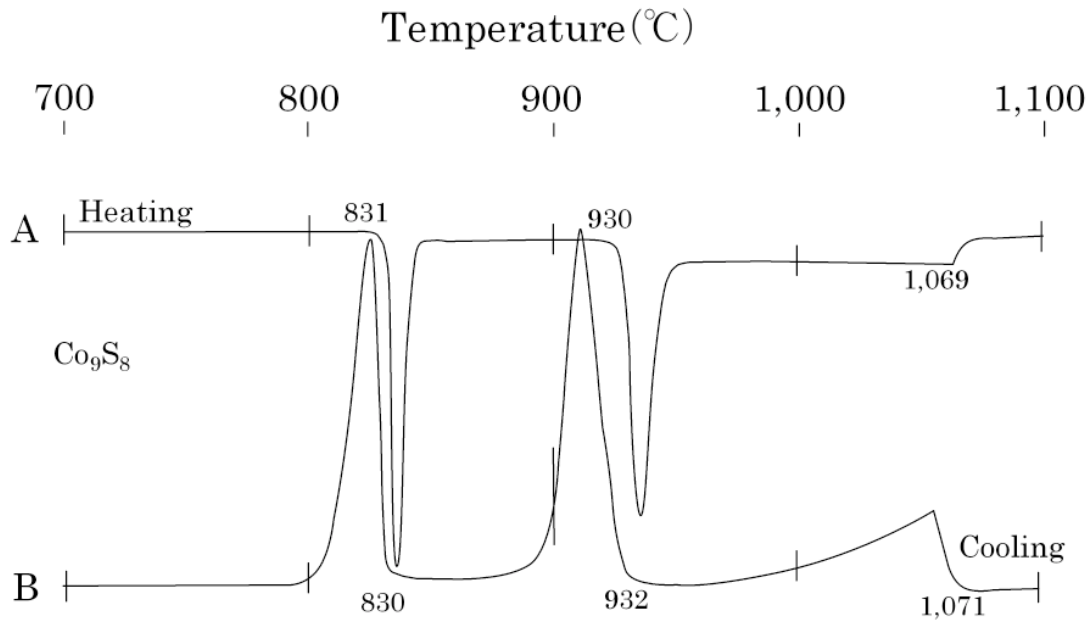

FIG. 10. DTA curves for synthetic cobalt pentlandite (and its high form), of composition Co_9S_8. A. Heating curve at 2°C/min. B. Cooling curve at the spontaneous cooling rate (~5°C/min) of the furnace.

ing) of the high form of the solid solution to monosulfide solid-solution + liquid. The continuous reactions in the temperature ranges from 865° ± 3°C to 982° ± 5°C ($Fe_{4.5}Ni_{4.5}S_8$) and from 930° ± 3°C to 1069° ± 5°C (Co_9S_8) with increasing Co content correspond to successive melting of monosulfide solid-solution, which is a breakdown product of the high-form solid-solution. Finally, the remnant monosulfide solid-solution melts completely at temperatures from 982° ± 5°C ($Fe_{4.5}Ni_{4.5}S_8$) to 1069° ± 5°C (Co_9S_8) with increasing Co content.

The high–low inversion of pentlandite and cobalt pentlandite end-members of the solid solution appears as a distinct reaction with a sharp single peak (T_1) in the DTA curves. It corresponds to a non-mass-transfer inversion. On the other hand, that of the solid-solution compositions appears as a shoulder peak broadening over some temperature range (maximum 38°C) from T_1 to T_2 in the curves. In this case, the inversion begins at T_1, continues with increasing temperature, and finishes at T_2. Thus, high- and low-form members of the solid solution coexist as "halfway" products of the phase transition at temperatures between T_1 and T_2. This inversion seems to be a mass-transfer type. The coexistence of both members of the solid solution was ascertained by using high-temperature X-ray powder-diffraction.

THE PENTLANDITE – COBALT PENTLANDITE SOLID-SOLUTION AND ITS HIGH FORM

The unit-cell constants for the solid solution with compositions between pentlandite ($Fe_{4.5}Ni_{4.5}S_8$) and cobalt pentlandite (Co_9S_8), synthesized at 500°C by the evacuated-silica-tube method and then cooled in air, were obtained at room temperature with a Guinier–Johansson camera using monochromatic Cu$K\alpha_1$ at 1.540598 Å (40 kV, 15 mA). Results are recorded in Table 9. The values of the cell constants decrease linearly with increasing Co content, from 10.0608(2) Å for pentlandite to 9.9287(2) Å for cobalt pentlandite (Fig. 11). The data of Kojonen (1976) and Knop & Ibrahim (1961) at room temperature also are shown in the figure, as are the values of *a* for the solid-solution series at 200°, 400° and 600°C, obtained with the high-temperature diffractometer in this study (Table 9). The high-temperature cell constants are approximately parallel to those at room temperature, but have larger values of *a*. These data indicate that there is a continuous solid-solution between pentlandite and cobalt pentlandite below 600°C. This inference also is supported by the linear increases of the reflectance values (Fig. 1) and temperature of inversion (Table 8, Fig. 9) with increasing Co content.

As mentioned above, the high-temperature X-ray-diffraction data demonstrate that the high form of cobalt pentlandite has a primitive cubic cell with *a* equal to 5.171(2) Å at 850°C, corresponding to *a*/2 of low-form cobalt pentlandite, similar to the high form of pentlandite (Sugaki & Kitakaze 1998). The relations between the *a* cell dimension and the compositions of the high-form solid-solution were also obtained at 750°, 800°, 850° and 900°C (Table 10, Fig. 12). The values of *a* decrease linearly with increasing Co content. Those data also indicate that a continuous high-form solid-solution between $Fe_{4.5}Ni_{4.5}S_8$ and Co_9S_8 exists as a stable phase at temperatures from 831° to 865°C.

A conspicuous thermal expansion of the pentlandite – cobalt pentlandite solid-solution is observed (Figs. 6, 7; Sugaki & Kitakaze 1998). Using the majority of the high-temperature cell-constant data for that solid solution and high form, the coefficient of linear expansion has been calculated (Table 11). The values for end-member pentlandite and cobalt pentlandite are 13.4×10^{-5} °C^{-1} (25° to 600°C) and 10.5×10^{-5} °C^{-1} (25° to 825°C), respectively. The former value is in good agreement with the values of 13.5×10^{-5} °C^{-1} (25° to 608°C) obtained by Morimoto & Kullerud (1964), and 13.4×10^{-5} °C^{-1} (25° to 580°C) obtained by Sugaki & Kitakaze (1998) for synthetic pentlandite of composition $Fe_{4.5}Ni_{4.5}S_{7.8}$, but larger than 11.1×10^{-5} °C^{-1} (24° to 200°C) for pentlandite from Frood, Sudbury, studied by Rajamani & Prewitt (1975b). The value for cobalt pentlandite is smaller than that of pentlandite. Those of the members of the solid solution are intermediate between the two end-members, and become smaller linearly with increasing Co content (Table 11, Fig. 13). On the other hand, the values for the high-form solid-solution series are smaller than those of the low-form series for the same composition, and also decrease linearly with increasing Co content.

TABLE 9. CELL CONSTANT OF PENTLANDITE – COBALT PENTLANDITE SOLID-SOLUTION OBTAINED BY GUINIER–JOHANSSON CAMERA AT ROOM TEMPERATURE AND BY HIGH-TEMPERATURE X-RAY DIFFRACTOMETER AT 200°, 400° AND 600°C

Mole % Co_9S_8	Room temperature *a* (Å)	200°C *a* (Å)	400°C *a* (Å)	600°C *a* (Å)
0	10.0608(2)	10.178(2)	10.312(2)	10.446(2)
10	10.0438(2)	10.165(2)	10.295(2)	10.424(2)
20	10.0335(2)	10.153(2)	10.278(2)	10.404(2)
30	10.0208(2)	10.140(2)	10.261(2)	10.382(2)
40	10.0075(2)	10.123(2)	10.244(2)	10.360(2)
50	9.9925(2)	10.105(2)	10.227(2)	10.338(2)
60	9.9783(2)	10.080(2)	10.210(2)	10.318(2)
70	9.9689(2)	10.065(2)	10.183(2)	10.296(2)
80	9.9531(2)	10.060(2)	10.171(2)	10.274(2)
90	9.9418(2)	10.045(2)	10.149(2)	10.254(2)
100	9.9287(2)	10.025(2)	10.135(2)	10.232(2)

TABLE 10. CELL CONSTANT OF THE HIGH FORM OF THE SOLID SOLUTION ALONG THE JOIN $Fe_{4.5}Ni_{4.5}S_8$ – Co_9S_8, AS OBTAINED WITH AN IP DIFFRACTOMETER AT 750°, 800°, 850° AND 900°C

Mole % Co_9S_8	750°C *a* (Å)	800°C *a* (Å)	850°C *a* (Å)	900°C *a* (Å)
0	5.282(2)	5.307(2)	5.335(2)	
10	5.261(2)	5.289(2)	5.312(2)	
20	5.248(2)	5.271(2)	5.298(2)	
30	5.233(2)	5.259(2)	5.282(2)	
40	5.220(2)	5.244(2)	5.270(2)	
50	5.204(2)	5.224(2)	5.255(2)	
60		5.209(2)	5.235(2)	
70		5.193(2)	5.215(2)	5.237(2)
80		5.181(2)	5.202(2)	5.224(2)
90			5.185(2)	5.207(2)
100			5.171(2)	5.191(2)

Phase Relations Along the Join $Fe_{4.5}Ni_{4.5}S_8$ – Co_9S_8 Above 400°C

The phase relations of the join $Fe_{4.5}Ni_{4.5}S_8$ – Co_9S_8 in the system Fe–Ni–Co–S at temperatures from 400° to 1100°C were derived from the combined data of equilibrium synthesis experiments (Table 12), EPMA (Tables 3, 4, and 5), high-temperature X-ray diffraction (Tables 6, 7 and 13) and DTA (Table 8), as shown in Figure 14. [Note that Tables 12 to 16 are available from the Depository of Unpublished Data, CISTI, National Research Council of Canada, Ottawa, Ontario K1A 0S2]. Among them, the high-temperature X-ray-diffraction data have exerted a major role in this study because all the high forms of pentlandite, cobalt pentlandite and members of the solid-solution series are unquenchable. In particular, a succession of high-temperature diffraction patterns of the monophase (Table 13) were tried at different temperatures from 3° to 50°C intervals to pinpoint phase boundaries for the phase diagram shown in Figure 14. Those were indispensable, together with DTA results, to draw the phase diagram for this join.

TABLE 11. THE VALUES OF THE LINEAR EXPANSION COEFFICIENT AS A FUNCTION OF COMPOSITION OF THE LOW- AND HIGH-FORM SOLID-SOLUTION ALONG THE JOIN $Fe_{4.5}Ni_{4.5}S_8$ – Co_9S_8 JOIN

Mole % Co_9S_8	Expansion coefficient (10^{-5} °C^{-1})	Temp. range (°C)	Expansion coefficient (10^{-5} °C^{-1})	Temp. range (°C)
	Low-form solid solution		**High-form solid solution**	
0	13.4	25–600	10.6	700–850
10	13.2	25–600	10.5	750–850
20	12.5	25–600	10.3	700–850
30	12.4	25–620	10.1	700–850
40	12.2	25–660	9.9	725–850
50	12.0	25–680	9.7	740–850
60	11.8	25–700	9.5	760–850
70	11.5	25–700	9.3	780–900
80	11.3	25–750	9.1	800–900
90	11.1	25–750	8.9	820–900
100	10.5	25–825	8.7	850–925

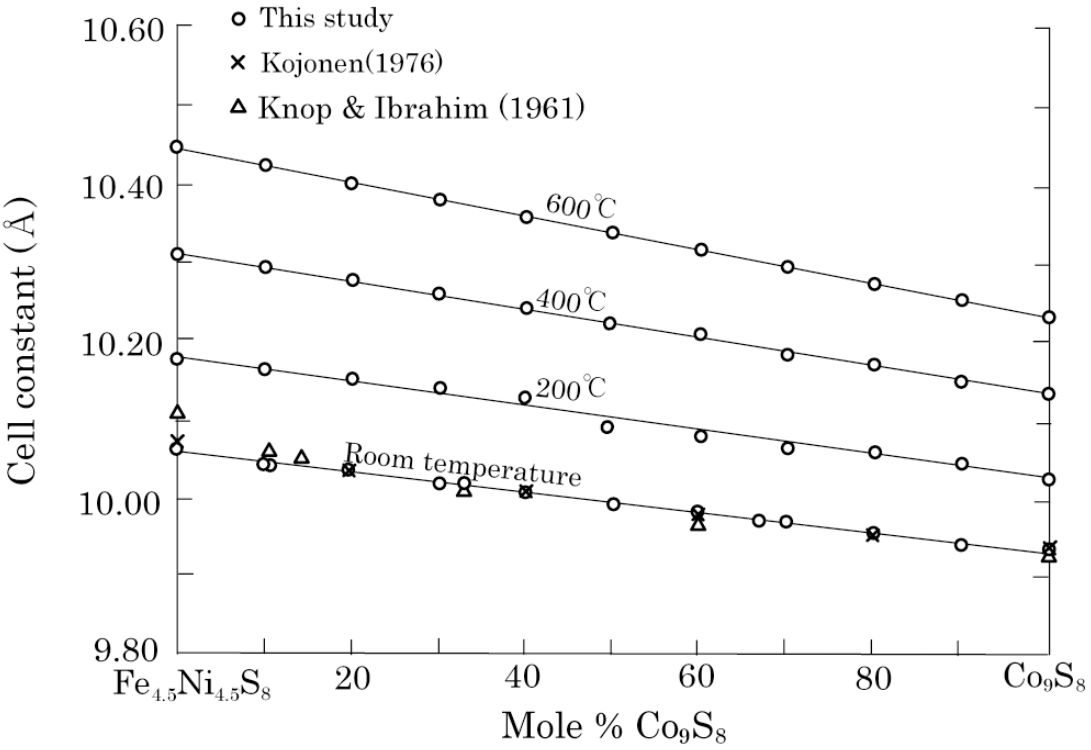

FIG. 11. The relationships between the cell constant and composition of the pentlandite – cobalt pentlandite solid-solution at room temperature, 200°, 400° and 600°C, together with the data of Knop & Ibrahim (1961) and Kojonen (1976).

There is a continuous solid-solution series (low form) between pentlandite and cobalt pentlandite below 615° ± 3°C, at which temperature pentlandite with the composition $Fe_{4.5}Ni_{4.5}S_{7.9}$ transforms into its high form (Sugaki & Kitakaze 1998). Also, a complete series of high-form compositions exists between the end members as stable phases above 831° ± 3°C, at which temperature cobalt pentlandite inverts to its high form. A two-phase field of coexisting low- and high-form members of the solid-solution series, extending over all the compositions of the join except for both end-members, appears as a loop in the temperature range from 615° to 831° ± 3°C with increasing Co content. Because of the presence of the two-phase field of coexisting low- and high-form phases, the inversion occurs over a temperature range that has a maximum interval of 38°C at the composition with 50 mole % Co_9S_8.

The high-form solid-solution series breaks down to a mixture of monosulfide solid-solution and liquid at temperatures from 865° ± 3°C (high-form pentlandite) to 930° ± 3°C (high-form cobalt pentlandite), the temperature increasing with increasing Co content along the series. A two-phase field of monosulfide solid-solution and liquid is found above these temperatures (Fig. 15). Finally, the remnant monosulfide solid-solution melts entirely at temperatures from 982° ± 5°C ($Fe_{4.5}Ni_{4.5}S_8$) to 1069° ± 5°C (Co_9S_8) with increasing Co content. According to the EPMA data (Table 5) for monosulfide solid-solution and liquid in the two-phase field, the values of the ratio Co/(Fe + Ni + Co) in monosulfide solid-solution are smaller than those of the original high-form member of the series, whereas those of the liquid are more Co-rich than the high-form member of the series, as shown in Figure 15. Because this figure is a projection from the sulfur corner into the Fe–Ni–Co base of the tetrahedron, the sulfur contents of monosulfide solid-solution and liquid are not shown. Monosulfide solid-solution is located at a higher sulfur content of about 50 atomic % S in the tetrahedron, whereas liquid is at a lower S content, about 45 atomic % S, with respect to the S content of the original bulk-composition. Of course, both of these phases are out of the plane Fe_9S_8 – Ni_9S_8 – Co_9S_8 and are in a pseudobinary relation with the original member of the solid solution (high form). The solid solution crystallizes as the high form by a pseudoperitectic reaction between monosulfide solid-solution and liquid at temperatures from 865° ± 3°C to 930° ± 3°C on the join $Fe_{4.5}Ni_{4.5}S_8$ – Co_9S_8.

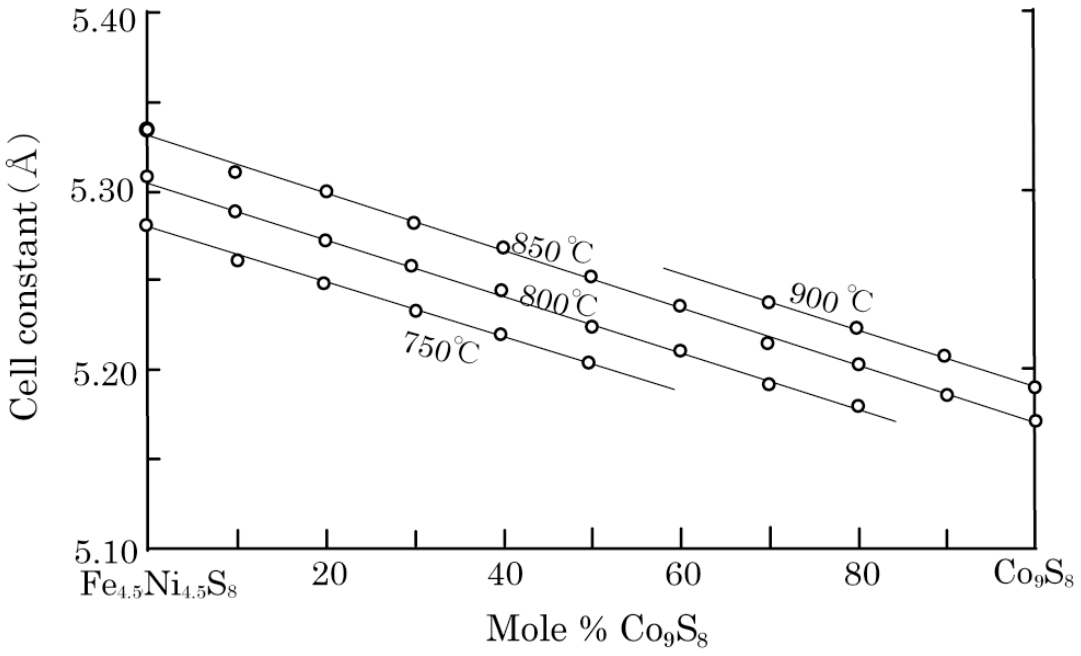

FIG. 12. The relationships of the unit-cell edge *versus* the compositions of the high form of the solid solution along in the $Fe_{4.5}Ni_{4.5}S_8$ – Co_9S_8 join at 750°, 800°, 850° and 900°C.

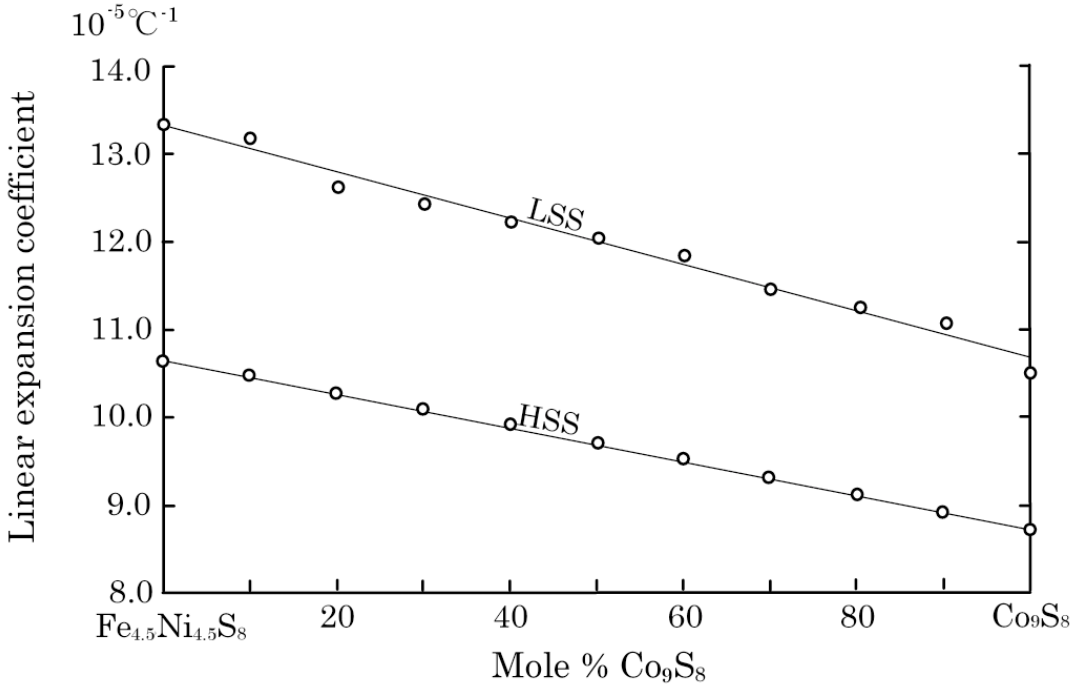

FIG. 13. The relationship of the linear expansion coefficients *versus* composition of the low and high forms of the solid solution along the join $Fe_{4.5}Ni_{4.5}S_8$ – Co_9S_8. See Table 1 for symbols.

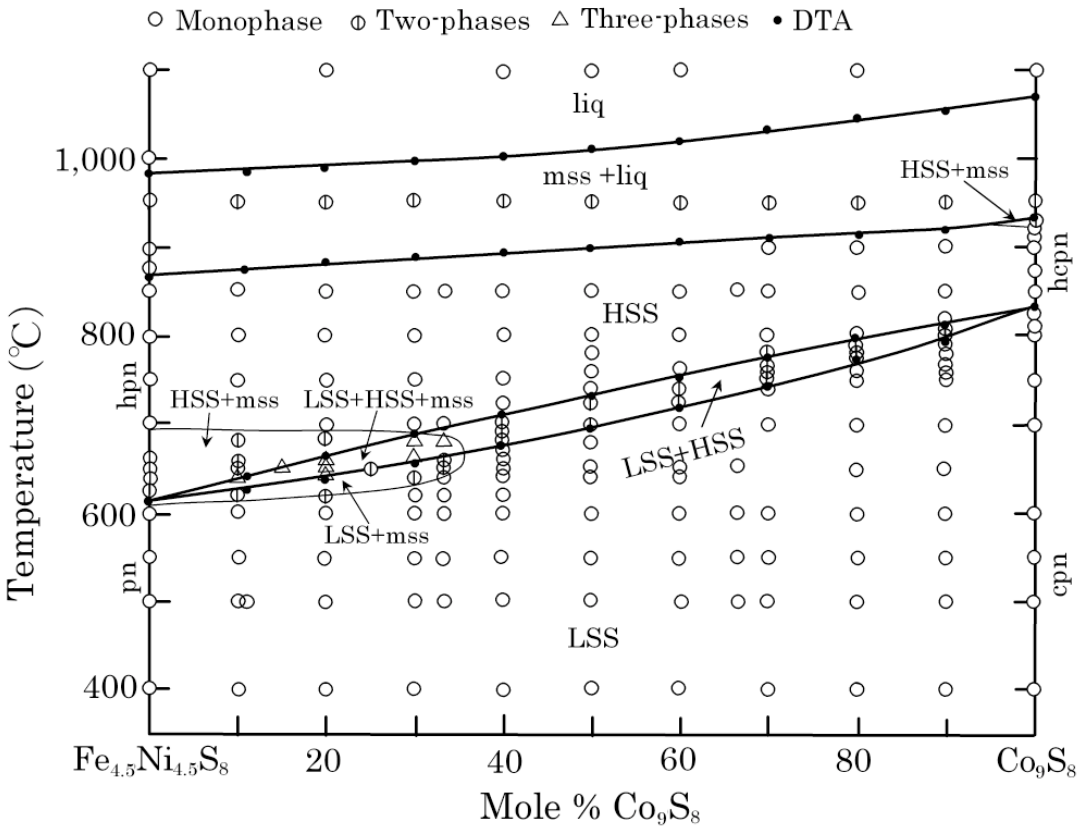

FIG. 14. The phase diagram for the join $Fe_{4.5}Ni_{4.5}S_8$ – Co_9S_8 at temperatures between 400° and 1100°C. See Table 1 for symbols; liq: liquid.

An extensive area in the phase diagram (Fig. 14) is occupied by both the pentlandite – cobalt pentlandite solid-solution and its high-form equivalents as single-phase fields. However, low- and high-form pentlandite and members of the series with less than approximately 35 mole % Co_9S_8 coexist with small amounts of monosulfide solid-solution in a limited field around 610° to 680°C (Fig. 14). Accordingly, there are on a local scale in the phase diagram two-phase fields of low- or high-form solid-solution phases coexisting with small amounts of monosulfide solid-solution and a three-phase field of coexisting low- and high-form solid-solution with small amounts of monosulfide solid-solution. The presence of the monosulfide solid-solution results in slightly more metal-rich compositions than (Fe + Ni + Co)/S = 9/8 for coexisting pentlandite, its high form, and low- and high-form members of the solid solution in the limited ranges of composition and temperature as above (Sugaki & Kitakaze 1998). In the same way, small amounts of cobalt monosulfide ($Co_{1-x}S$), which is an end-member of monosulfide solid-solution, appear as inclusions in high-form cobalt pentlandite at 928° ± 3°C because high-form cobalt pentlandite becomes slightly more Co-rich than Co/S = 9/8. Thus a very small two-phase field of high-form cobalt pentlandite (or solid solution) + cobalt monosulfide (or monosulfide solid-solution) occurs locally.

THE EXTENT OF THE $Fe_{4.5}Ni_{4.5}S_8$ – Co_9S_8 SOLID-SOLUTION IN THE QUATERNARY SYSTEM Fe–Ni–Co–S

The extent of the high-form solid-solution at 850°C

The continuous series of high- and low-form solid-solution phases expand to both the Fe- and Ni-enriched sides with respect to the compositions along the join $Fe_{4.5}Ni_{4.5}S_8$–Co_9S_8. The high-form solid-solution extends as an elongate cylindroidal shape with a lenticular section from Co-free high-form pentlandite on the Fe–Ni–S face toward the Co_4S_3 – Co_9S_8 solid-solution (Kitakaze & Sugaki 2003) on the Co–S edge of the qua-

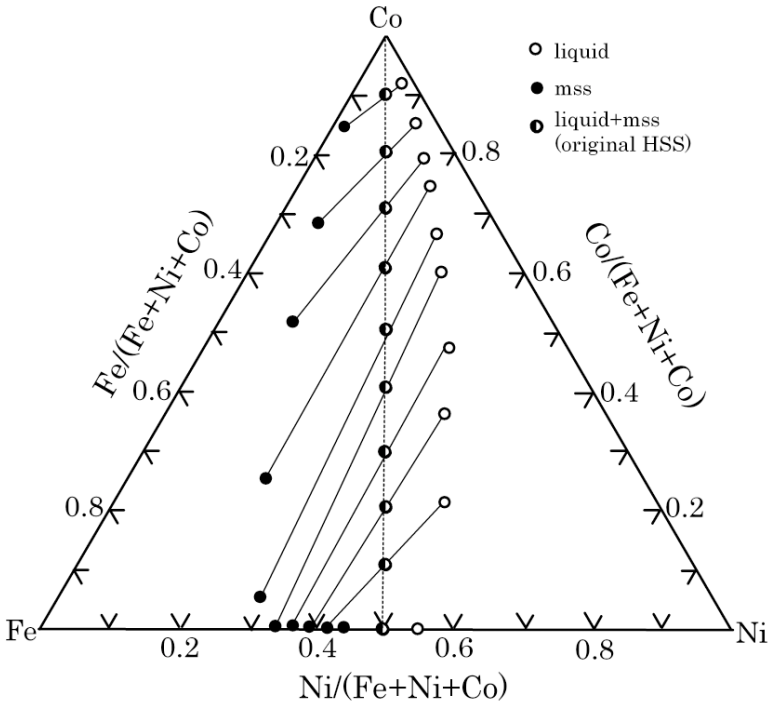

FIG. 15. The compositions of monosulfide solid-solution and liquid coexisting in the two-phase field along the join $Fe_{4.5}Ni_{4.5}S_8$ – Co_9S_8 at 950°C (Table 5). The compositions are projected onto the Fe–Ni–Co base from the S corner of the tetrahedron.

ternary system Fe–Ni–Co–S (tetrahedron) at 850°C (Fig. 16). Most of the products for the starting bulk-compositions containing 0, 10, 20, 33.33 and 66.67 mole % Co_9S_8 along the three joins $Fe_{5.0}Ni_{4.0}S_8$, $Fe_{4.5}Ni_{4.5}S_8$ or $Fe_{4.0}Ni_{5.0}S_8$ – Co_9S_8 appear as a monophase solid-solution of high form except for $Fe_{4.0}Ni_{5.0}S_8$ (Table 14, deposited). However, all the products along the join $Fe_{5.5}Ni_{3.5}S_8$ – Co_9S_8 on the more Fe-rich side than the joins mentioned above are a mixture of high-form solid-solution and small amounts of monosulfide solid-solution and liquid. In this case, the compositions of the high-form solid-solution, such as $Fe_{5.19}Ni_{3.91}S_{7.90}$, $Fe_{4.56}Ni_{3.55}Co_{0.90}S_{7.99}$, $Fe_{4.05}Ni_{3.15}Co_{1.80}S_{8.00}$, $Fe_{3.40}Ni_{2.62}Co_{2.99}S_{7.99}$ and $Fe_{1.68}Ni_{1.31}Co_{6.02}S_{7.99}$ obtained by EPMA (Table 14, deposited) correspond to those of the Fe-rich margin of the solid-solution field. Similarly, the products for the starting compositions with $Fe_{4.0}Ni_{5.0}S_8$ and 10, 20 and 33.33 mole % Co_9S_8 along the join $Fe_{3.5}Ni_{5.5}S_8$ – Co_9S_8 on the more Ni-rich side than the joins listed above, also are a mixture of high-form solid-solution, monosulfide solid-solution and liquid. The compositions of these high-form solid-solutions, such as $Fe_{3.79}Ni_{6.32}S_{7.99}$, $Fe_{3.37}Ni_{4.76}Co_{0.90}S_{7.97}$, $Fe_{2.99}Ni_{4.23}Co_{1.00}S_{7.98}$ and $Fe_{2.46}Ni_{3.54}Co_{3.01}S_{7.99}$ (Table 14, deposited) indicate those of the Ni-rich margin of the field of solid solution. The high-form solid-solution coexists with monosulfide solid-solution or liquid (or both) at 850°C, but cannot coexist with γ(Fe,Ni,Co) owing to the appearance of an extensive field of liquid, except for a Co-rich portion of the solid-solution series (Fig. 16).

The extent of the low-form solid-solution at 500°C

The extension of the low-form solid-solution (pentlandite – cobalt pentlandite solid-solution) in the tetrahedron Fe–Ni–Co–S at 500°C is shown in Figure 17. We rely on the data of Shewman & Clark (1970), Misra & Fleet (1973), Sugaki & Kitakaze (1996, and unpubl. data) and Peregoedova & Ohnenstetter (2002) for the system Fe–Ni–S, of Lamprecht (1978) for the system Ni–Co–S, of Raghavan (1988) for the system Fe–Co–S, and on Knop *et al*. (1965), Kaneda *et al*. (1986) and this work for the system Fe–Ni–Co–S. The low-form solid-solution extends continuously from Co-free pentlandite, which has a considerable compositional range from $Fe_{6.15}Ni_{2.94}S_{7.91}$ to $Fe_{2.43}Ni_{6.56}S_{8.01}$, including $Fe_{4.5}Ni_{4.5}S_8$ on the Fe–Ni–S face at 500°C, to cobalt pentlandite Co_9S_8 on the Co–S edge of the tetrahedron so as to occupy all the Co-rich portion of the Fe_9S_8 – Ni_9S_8 – Co_9S_8 plane, namely, the $(Fe,Ni,Co)_9S_8$ plane

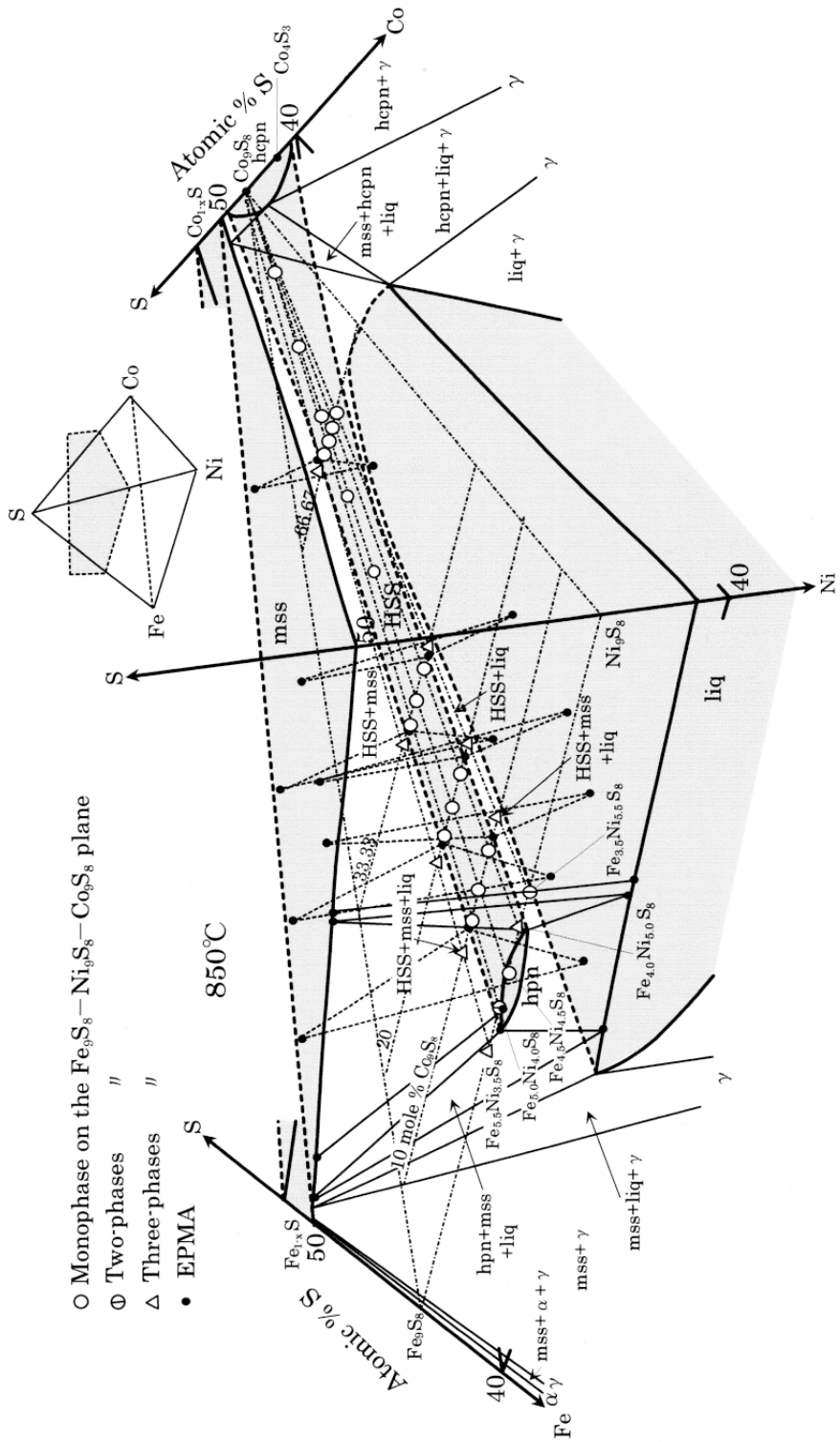

FIG. 16. The phase diagram shows an extensive field of the high-form solid-solution $(Fe,Ni,Co)_9S_8$ and its phase assemblages with monosulfide solid-solution, α, γ or liquid (or both) in the quaternary system Fe–Ni–Co–S at 850°C. See Table 1 for symbols; liq: liquid.

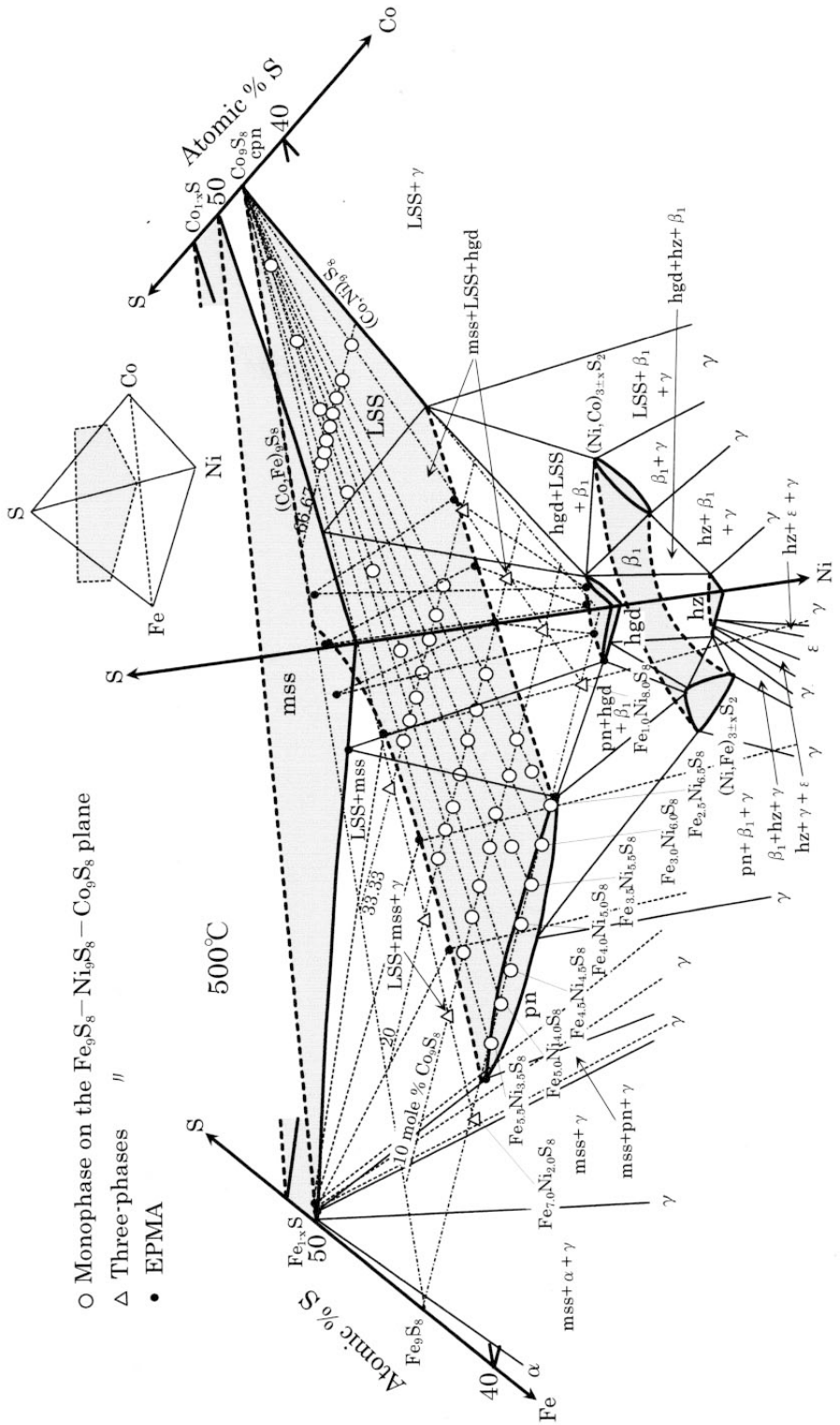

FIG. 17. Extent of the pentlandite – cobalt pentlandite solid-solution (low form) $(Fe,Ni,Co)_9S_8$ and its phase assemblages with monosulfide solid-solution, high godlevskite, β_1, heazlewoodite, α or γ (or both) in the Fe–Ni–Co–S tetrahedron at 500°C. See Table 1 for symbols.

from $(Co,Ni)_9S_8$ to $(Co,Fe)_9S_8$ (Fig. 17). This solid-solution series is invariably associated with monosulfide solid-solution along the sulfur-rich side of the tetrahedron. The Ni-rich portion of the solid solution coexists with $\beta_1(Ni,Fe)_{3\pm x}S_2$ (Lin *et al.* 1978, Kitakaze & Sugaki 2001, Sugaki & Kitakaze, unpubl. data) or Co-bearing high godlevskite, $(Ni,Fe,Co)_7S_6$, or both. On the other hand, the Co-rich part of the solid solution is associated with $\gamma(Co,Ni,Fe)$, $\beta_1(Ni,Co,Fe)_{3\pm x}S_2$ or Co-bearing high godlevskite. The products for the starting compositions with 0, 10, 20, 33.33, and 66.67 mole % Co_9S_8 along the seven joins having as end points $Fe_{5.5}Ni_{3.5}S_8$, $Fe_{5.0}Ni_{4.0}S_8$, $Fe_{4.5}Ni_{4.5}S_8$, $Fe_{4.0}Ni_{5.0}S_8$, $Fe_{3.5}Ni_{5.5}S_8$, $Fe_{3.0}Ni_{6.0}S_8$ or $Fe_{2.5}Ni_{6.5}S_8$ are all a single phase of the low-form (pentlandite) solid-solution. On the other hand, those products for the compositions with 0, 10, 20 and 33.33 mole % Co_9S_8 along the join $Fe_{7.0}Ni_{2.0}S_8$ – Co_9S_8 are a mixture of low-form solid-solution and small amounts of monosulfide solid-solution and $\gamma(Fe,Ni,Co)$. In this case, the compositions of the low-form solid-solution, such as $Fe_{6.15}Ni_{2.94}S_{7.91}$, $Fe_{5.64}Ni_{1.96}Co_{1.39}S_{8.01}$, $Fe_{4.49}Ni_{2.04}Co_{2.45}S_{8.02}$ and $Fe_{3.85}Ni_{1.63}Co_{3.50}S_{8.02}$, obtained with EPMA (Table 15, deposited) correspond to those of the Fe-rich margin of the solid-solution field at 500°C. Similarly, the products for the same compositions as above along the $Fe_{1.0}Ni_{8.0}S_8$ – Co_9S_8 join are a mixture of low-form solid-solution, monosulfide solid-solution and Co-bearing high godlevskite, and the EPMA compositions of the low-form solid-solution, such as $Fe_{2.43}Ni_{6.56}S_{8.01}$, $Fe_{1.63}Ni_{5.64}Co_{1.72}S_{8.01}$, $Fe_{1.14}Ni_{5.40}Co_{2.47}S_{7.99}$, and $Fe_{0.73}Ni_{5.00}Co_{3.26}S_{8.01}$ (Table 15, deposited) define the Ni-rich boundary of the solid-solution field.

The extent of both the solid solutions with the inversion zone at 650°C

The extent and coexistence of both the high- and low-form solid-solutions in the quaternary system at 650°C are shown in Figure 18, based on the data of Lamprecht (1976), Sugaki & Kitakaze (1996) and this work (Table 16, deposited). As seen in the figure, the high-form solid-solution appears as a wedge-like shape on the side containing less than about 8 to 18 mole % Co_9S_8 in the $(Fe,Ni,Co)_9S_8$ plane of the tetrahedron, whereas the low-form solid-solution comes out as a triangular form with an apex of Co_9S_8 on the side richer in Co than approximately 18 to 24 mole % Co_9S_8 in the plane. Between them, we found a lenticular area of coexistence of the high- and low-form solid-solutions in an inversion zone. This area corresponds to a "halfway" zone of the phase transition. The S-rich surface (boundary) of the high- or low-form compositions with less than approximately 35 mole % Co_9S_8 (Fig. 14) becomes somewhat less enriched than those of the $(Fe,Ni,Co)_9S_8$ plane (Fig. 18). Accordingly, the surface of the solid solution separates slightly from the $(Fe,Ni,Co)_9S_8$ plane and is less enriched than the plane in the tetrahedron. The high-form solid-solution, as above, invariably coexists with a small amount of monosulfide solid-solution on the $(Fe,Ni,Co)_9S_8$ plane at 650°C. Similarly, the monosulfide solid-solution appears slightly in a coexisting area (inversion zone) of high- and low-form solid-solution between about 8 and 24 mole % Co_9S_8 and a field of solid solution containing less Co than about 35 mole % Co_9S_8 on the $(Fe,Ni,Co)_9S_8$ plane (Fig. 18). All the products for starting materials with 0, 10, 20, 33.33 and 66.67 mole % Co_9S_8 along the join $Fe_{5.5}Ni_{3.5}S_8$ – Co_9S_8 at 650°C are three-phase assemblages of high- or low-form solid-solution, monosulfide solid-solution and $\gamma(Fe,Ni,Co)$ (Table 16, deposited). In this case, the compositions of $Fe_{5.42}Ni_{3.64}S_{7.94}$ and $Fe_{4.69}Ni_{3.42}Co_{0.94}S_{7.97}$ for 0 and 10 mole % Co_9S_8, respectively, as the high-form solid-solution, and $Fe_{4.20}Ni_{3.03}Co_{1.80}S_{7.97}$, $Fe_{3.54}Ni_{2.47}Co_{2.99}S_{8.00}$ and $Fe_{1.76}Ni_{1.24}Co_{6.00}S_{8.00}$ for 20, 33.33 and 66.67 mole % Co_9S_8, respectively, as the low-form solid-solution on the join, indicate the Fe-rich end of these solid solutions. On the other hand, the Ni-rich high-form solid-solution containing 0 and 10 mole % Co_9S_8 join β_2 with $Ni_{4\pm x}S_3$ on the Ni–S edge (Sugaki & Kitakaze 1996) and β_2 with $(Ni,Co)_{4\pm x}S_3$ on the Ni–Co–S face, respectively, of the tetrahedron. However, the Ni-rich ends of the low-form solid-solution, with 33.33 mole % Co_9S_8, have the compositions $Fe_{0.19}Ni_{6.61}Co_{2.24}S_{8.01}$ and $Fe_{0.14}Ni_{5.62}Co_{3.25}S_{7.99}$, respectively located inside the tetrahedron, although very close to the Ni–Co–S face (Fig. 18). Also, the Co-rich low-form solid-solution near Co_9S_8 reaches the Ni–Co–S face to join $(Co,Ni)_9S_8$ (Lamprecht 1978).

Inversion temperatures of the $(Fe,Ni,Co)_9S_8$ solid-solution with an extended field as mentioned above have been examined in detail using DTA. We found two kinds of peaks for the high–low inversion of the solid solution, namely the sharp single peak (T_1 for $Fe_{4.5}Ni_{4.5}S_8$ and Co_9S_8 in Fig. 9), and a broad peak with a shoulder (T_1 and T_2 for the solid solution from 20 to 80 mole % Co_9S_8 in Fig. 9). The phase transition of its S-rich marginal end (boundary), in addition to that in the end members, appears as a single peak, which indicates a non-mass-transfer inversion. The other compositions show a broad, continuous peak from T_1 to T_2 (Table 8); these inversions correspond to the mass-transfer type. We found a tendency for the temperature of the high–low inversion of the $(Fe,Ni,Co)_9S_8$ solid-solution to increase with increasing Co, Fe or S contents and to decrease with increasing Ni or S contents (or both). For example, the temperatures (T_1) of the single-peak reaction (non-mass- transfer inversion) for the compositions of the low-form solid-solution, which are a single-phase product at 500°C, are as follows: 597° ± 3°C for $Fe_{2.50}Ni_{6.50}S_{8.00}$, 602° ± 3°C for $Fe_{3.00}Ni_{6.00}S_{8.00}$, 608° ± 3°C for $Fe_{2.25}Ni_{5.85}Co_{0.90}S_{8.00}$, 610° ± 3°C for $Fe_{3.50}Ni_{5.50}S_{8.00}$, 613° ± 3°C for $Fe_{4.00}Ni_{5.00}S_{8.00}$, 615° ± 3°C for $Fe_{4.50}Ni_{4.50}S_{8.00}$, 617° ± 3°C for $Fe_{5.00}Ni_{4.00}S_{8.00}$, 618° ± 3°C for $Fe_{2.00}Ni_{5.20}Co_{1.80}S_{8.00}$, 632° ± 3°C for $Fe_{1.67}Ni_{4.33}Co_{3.00}S_{8.00}$, 645 ± 3°C for

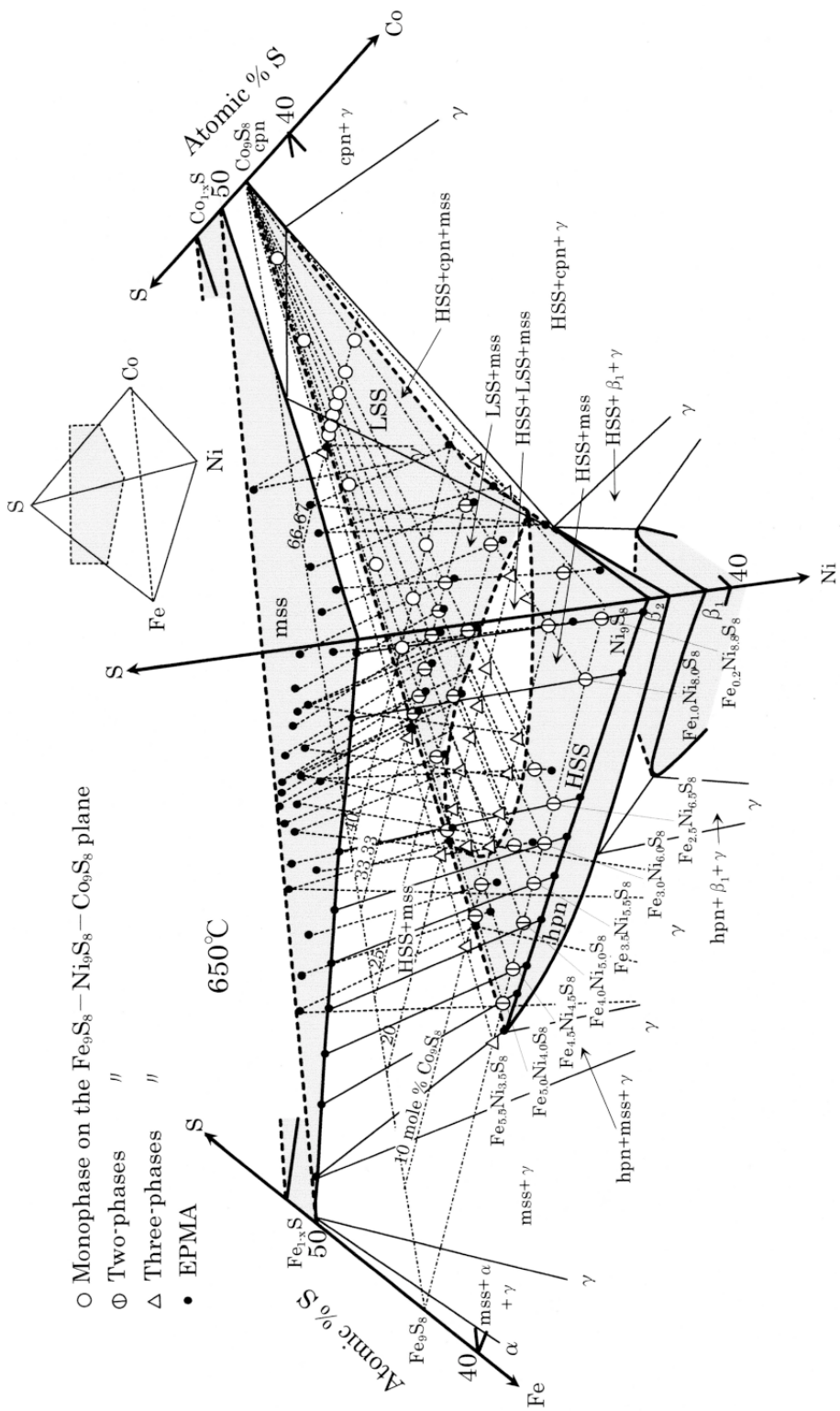

FIG. 18. The phase diagram illustrates the appearance of extensive high- and low-form solid-solution and their phase assemblages with monosulfide solid-solution, β_1, α or γ (or both) in the quaternary system Fe–Ni–Co–S at 650°C. We found a zone of coexisting high- and low-form solid-solutions between their wide fields. Also, because the S-rich boundary of solid-solution compositions with less than approximately 35 mole % Co_9S_8 becomes slightly poorer in S than those in the $(Fe,Ni,Co)_9S_8$ plane at this temperature, two- or three-phase assemblages of high- and low-form solid-solution with a small amount of monosulfide solid-solution appear in the $(Fe,Ni,Co)_9S_8$ plane. See Table 1 for symbols.

$Fe_{4.95}Ni_{3.15}Co_{0.90}S_{8.00}$, 667° ± 3°C for $Fe_{4.40}Ni_{2.80}Co_{1.80}S_{8.00}$, 693° ± 3°C for $Fe_{3.67}Ni_{2.33}Co_{3.00}S_{8.00}$, 720° ± 3°C for $Fe_{0.83}Ni_{2.17}Co_{6.00}S_{8.00}$, 778° ± 3°C for $Fe_{1.83}Ni_{1.17}Co_{6.00}S_{8.00}$, and 831° ± 3°C for Co_9S_8.

Discussion

Kullerud (1962, 1963) reported that pentlandite is present as a stable phase below 610° ± 3°C, but breaks down into a mixture of $Ni_{3\pm x}S_2$ and pyrrhotite (monosulfide solid-solution) at this temperature or above. However, Sugaki *et al*. (1982) and Sugaki & Kitakaze (1992, 1998) found that pentlandite transforms instead into the high form at 615° ± 3°C, and that it is stable up to 865° ± 3°C.

Sugaki *et al.* (1983, 1984) found that high-form pentlandite forms a continuous solid-solution with $Ni_{3\pm x}S_2$ at 650° to 800°C in the system Fe–Ni–S. Fedorova & Sinyakova (1993) reported high-form pentlandite solid-solution (heazlewoodite solid-solution in their terminology) at 820°C. Karup-Møller & Makovicky (1995) also described the existence of a continuous and extensive solid-solution $(Fe,Ni)_{3\pm x}S_2$, between high-form pentlandite and $Ni_{3\pm x}S_2$ at 725°C. Sugaki & Kitakaze (1996) ascertained that high-form pentlandite forms an extensive solid-solution with Ni_4S_3 (β_2), not $Ni_{3\pm x}S_2$ (β) (Lin *et al*. 1978, Singleton *et al*. 1990, Kitakaze & Sugaki 1996, 2001).

The thermal stability of cobalt pentlandite Co_9S_8 has been investigated in the binary system Co–S by many authors such as Friedrich (1908), Hülsmann & Weibke (1936), Lundqvist & Westgren (1938), Hansen & Anderko (1958), Elliott (1964), Kuznetsov *et al*. (1965), Lamprecht (1976, 1978), and Massalski *et al*. (1990). According to them, cobalt pentlandite is stable up to about 833°C (Massalski *et al*. 1990), but breaks down to a mixture of Co_4S_3 and cobalt monosulfide ($Co_{1-x}S$) at this temperature or above, and the Co_4S_3 produced breaks down further into a mixture of cobalt monosulfide + liquid at 932°C (Massalski *et al*. 1990). Rosenqvist (1954), Rau (1976) and Chen & Chang (1978) determined the activity of S in $Co_{4\pm x}S_3$, Co_9S_8 and $Co_{1-x}S$ along the binary join Co–S using H_2/H_2S gas mixtures at high temperatures, and found that Co_9S_8 breaks down to $Co_{4\pm x}S_3$ and $Co_{1-x}S$ at 830°C or above.

Kitakaze & Sugaki (1992, this study) found that cobalt pentlandite does undergo a phase change at 831° ± 3°C, but in disagreement with the above, does not break down. Instead, it inverts into the high form at this temperature. The high form of cobalt pentlandite is stable up to 930° ± 3°C, where it breaks down to a mixture of cobalt monosulfide (Fe- and Ni-free end-member of monosulfide solid-solution) and liquid in an incongruent melting reaction. Finally, remnant cobalt monosulfide melts completely at 1069° ± 5°C or above.

In the DTA investigation of the thermal stability of natural and synthetic pentlandite and Co-bearing pentlandite, Vaasjoki *et al*. (1974) found that their breakdown temperatures rose from 611° to 746°C with increasing Co content. Similarly, Kojonen (1976) reported that a continuous solid-solution is formed between pentlandite and cobalt pentlandite is formed at 570°C and breaks down at increasingly higher temperatures with Co content, from 610° for $Fe_{4.5}Ni_{4.5}S_8$ to 833°C for Co_9S_8, and then incongruently melts at 862° ($Fe_{4.5}Ni_{4.5}S_8$) to 932°C (Co_9S_8). They did not recognize the existence of the high form of the solid solution. The results of the present study make it clear that the high form of the continuous solid-solution between pentlandite and cobalt pentlandite is present as a stable phase. We further believe that pentlandite, cobalt pentlandite and the solid solution between them can crystallize as the high form during ore-forming processes in nature by a peritectic reaction between monosulfide solid-solution and sulfide liquid (sulfide magma) at about 800° to 900°C.

The high form of cobalt pentlandite is a newly recognized phase in the system Co–S. The recognition of this phase requires that the high-temperature, metal-rich portion of this binary system, especially the phase relations between $Co_{4\pm x}S_3$ and $Co_{1-x}S$, be re-examined. According to our preliminary work (Kitakaze & Sugaki 2003), there is a possibility that high-form cobalt pentlandite may form a solid solution with $Co_{4\pm x}S_3$ above 831°C. The data pertaining to this experiment will be reported separately.

Small amounts of monosulfide solid-solution coexist with low- and high-form pentlandite and the low and high forms of the solid solution in a limited field from 0 to about 35 mole % Co_9S_8 around 610° to 680°C, as had been already reported by Knop & Ibrahim (1961), Craig (1967), Kojonen (1976) and Kaneda *et al*. (1986). The published compositional and thermal ranges of the pentlandite solid-solution with monosulfide solid-solution are not entirely in agreement with each other or with our data. However, these discrepancies do not affect the stability relations of the solid solution between pentlandite and cobalt pentlandite.

Although the extent of the pentlandite – cobalt pentlandite solid-solution (low form) within the quaternary system Fe–Ni–Co–S was investigated by Knop *et al*. (1965) and Kaneda *et al*. (1986), we also examined the extent of the low-form solid-solution toward the more Fe- and Ni-rich sides of the join $Fe_{4.5}Ni_{4.5}S_8$ – Co_9S_8 in the tetrahedron Fe–Ni–Co–S at 500°C (Fig. 17). We furthermore studied the extent of the high-form solid-solution within the tetrahedron at 850°C (Fig. 16), and documented the phase relations among the solid solution, monosulfide solid-solution and γ, including the coexistence of high- and low-form solid-solutions at 650°C (Fig. 18).

On the other hand, the phase-equilibrium studies of the system Fe–Ni–Cu–S in relation with the genesis of Cu–Ni ore deposits were carried out by Craig & Kullerud (1969), Hill (1983), Hayashi (1985) and Peregoedova & Ohnenstetter (2002). The high-form

pentlandite or cobalt pentlandite extends as a solid solution inside the tetrahedron Fe–Ni–Cu–S from the Fe–Ni–S face. In fact, Peregoedova & Ohnenstetter (2002) found a continuous heazlewoodite – intermediate solid-solution (their terminology), which may correspond to our Co-free high-form pentlandite solid-solution at 760°C. But the other authors did not recognize such a solid solution, although they reported the stable assemblages of pentlandite or its high form, with chalcopyrite, bornite or intermediate solid-solution. The high- and low-form solid-solutions $(Fe,Ni,Co,Cu)_9S_8$ are important phases in the system Fe–Ni–Co–Cu–S. As such, their thermal stability, compositional fields and phase assemblages should be established definitively in phase diagrams in future.

Acknowledgements

We are deeply grateful to Steven D. Scott for his valuable comments and critical review of this paper and his correction of the English, and S. Farrell and A. Peregoedova for their critical reviews, valuable comments and suggestions. We also thank Robert F. Martin for his editorial care. This research was funded by a Grant-in-Aid for Scientific Research from the Ministry of Education, Culture, Sport, Science and Technology of Japan, to which the authors offer their sincere thanks.

References

Bence, A.E. & Albee, A.L. (1968): Empirical correction factors for the electron microanalysis of silicate and oxides. *J. Geol.* **76**, 382-403.

Chen, Y.O. & Chang, Y.A. (1978): Thermodynamics and phase relationships of transition metal–sulfur systems. 1. The cobalt–sulfur system. *Metall. Trans.* **9B**, 61-67.

Craig, J.R. (1967): Pentlandite composition. *Carnegie Inst. Wash., Yearbook* **65**, 329.

_____ & Kullerud, G. (1969): Phase relations in the Cu–Fe–Ni–S system and their application to magmatic ore deposits. *In* Magmatic Ore Deposits (H.D.B. Wilson, ed.). *Econ. Geol., Monogr.* **4**, 344-358.

Elliott, R. P. (1964): *Constitution of Binary Alloys* (first supplement). McGraw-Hill, New York, N.Y. (332).

Fedorova, Z.N. & Sinyakova, E.F. (1993): Experimental investigation of physicochemical conditions of pentlandite formation. *Russ. J. Geol. Geophys.* **34**, 79-87.

Fleet, M.E. (1972): The crystal structure of α-Ni_7S_6. *Acta Crystallogr.* **B28**, 1237-1241.

_____ (1977): The crystal structure of heazlewoodite, and metallic bonds in sulfide minerals. *Am. Mineral.* **62**, 341-345.

Friedrich, K. (1908): Über das Schmelzdiagramm der Kobalt – Schwefellegierungen. *Metallurgie* **5**, 212-215.

Geller, S (1962): Refinement of the crystal structure of Co_9S_8. *Acta Crystallogr.* **25**, 1195-1198.

Hansen, M. & Anderko, K. (1958): *Constitution of Binary Alloys* (2nd ed.). McGraw-Hill, New York, N.Y. (497-499).

Hayashi, T. (1985): *Study on the Phase Equilibrium in the System Cu–Fe–Ni–S, Especially Phase Relation in the Central Portion.* Doctoral thesis, Tohoku University, Sendai, Japan.

Hill, R.E.T. (1983): Experimental study of phase relations at 600°C in a portion of the Fe–Ni–Cu–S system and its application to natural sulphide assemblages. *In* Sulphide Deposits in Mafic and Ultramafic Rocks (D.L. Buchanan & M.J. Jones, eds.). Institute of Mining and Metallurgy, London, U.K. (14-21).

Hülsmann, O. & Weibke, F. (1936): Über die niederen Sulfide des Kobalts das Zustandsdiagramm des Systems Co–CoS. *Z. anorg. allg. Chem.* **227**, 113-123.

Kaneda, H., Takenouchi, S. & Shoji, T. (1986): Stability of pentlandite in the Fe–Ni–Co–S system. *Mineral. Deposita* **21**, 167-180.

Karup-Møller, S. & Makovicky, E. (1995): The phase system Fe–Ni–S at 725°C. *Neues Jahrb. Mineral., Monatsh.*, 1-10.

Kitakaze, A. & Sugaki, A. (1992): Phase transition of pentlandite – cobalt pentlandite series and its phase relations. *Proc. 29th Int. Geol. Congress* (*Kyoto*) **3**, 678 (abstr.).

_____ & _____ (1996): Study of the $Ni_{3\pm x}S_2$ in the Ni–S system, especially high-temperature forms of Ni_3S_2 and Ni_4S_3. *Joint Annual Meeting Japan. Assoc. Mineral. Petrol. Econ. Geol., Mineral. Soc. Japan & Soc. Resource Geol.* (*Kanazawa*), 149 (abstr.).

_____ & _____ (2001): Study of the $Ni_{3\pm x}S_2$ phase in the Ni–S system with emphasis on the phases of high-form Ni_3S_2 (β_1) and Ni_4S_3 (β_2). *Neues Jahrb. Mineral., Monatsh.*, 41-48.

_____ & _____ (2003): The phase relations in a metal-rich portion of the Co–S system above 700°C, especially reexamination of phase Co_4S_3. *Joint Meeting Mineral. Soc. Japan & Assoc. Mineral. Petrol. Econ. Geol.* (*Sendai*), 48 (abstr.).

Knop, O. & Ibrahim, M.A. (1961): Chalkogenides of the transition elements. II. Existence of the π phase in the M_9S_8 section of the system Fe–Co–Ni–S. *Can. J. Chem.* **39**, 297-317.

_____, _____ & Sutarno (1965): Chalcogenides of the transition elements. IV. Pentlandite, a natural π phase. *Can. Mineral.* **8**, 291-316.

KOJONEN, K. (1976): Experiments on synthetic pentlandite. *In* Ore Mineral Systems (G.H. Moh, ed.). *Neues Jahrb. Mineral., Abh*. **126**, 133-135.

KULLERUD, G. (1962): The Fe–Ni–S system. *Carnegie Inst. Wash., Yearbook* **61**, 144-150.

_____ (1963): Thermal stability of pentlandite. *Can. Mineral*. **7**, 353-366.

KUZNETSOV, V.G., SOKOLOVA, M A., PALKINA, K.K. & POPOVA, Z.V. (1965): The cobalt – sulfur system. *Izv. Akad. Nauk SSSR, Neorgan. Materialy* **1**, 675-689 (in Russ.). (English transl. *Russ. Inorg. Materials*, 1966, 617-632).

LAMPRECHT, G. (1976): Some new data on the Co–S system. *Neues Jahrb. Mineral., Abh*. **128**, 126-127.

_____ (1978): Phasengleichgewichte in System Co–Ni–S unterhalb 1,000°C. *Neues Jahrb. Mineral., Monatsh*., 176-191.

LIN, R.Y., HU, D.C. & CHANG, Y.A. (1978): Thermodynamics and phase relationships of transition metal–sulfur systems. II. The nickel–sulfur system. *Metall. Trans*. **9B**, 531-538.

LINDQVIST, M., LUNDQVIST, D. & WESTGREN, A. (1936): The crystal structure of Co_9S_8 and of pentlandite $(Ni,Fe)_9S_8$. *Svensk Kemist. Tidskrift* **48**, 156-160.

LINÉ, G. & HUBER, M. (1963): Étude radiocristallographique à haute température de la phase non stoechiométrique $Ni_{3\pm x}S_2$. *C.R. Acad. Sci. Paris* **256**, 3118-3120.

LUNDQVIST, D. & WESTGREN, A. (1938): Röntgenuntersuchung des Systems Co–S. *Z. anorg. Allg. Chem*. **239**, 85-88.

LUTTS, A. & GIELEN, P.M. (1970): The order–disorder transformation in $FeNi_3$. *Phys. Status Solidi* **41**, K81-84.

MASSALSKI, T.B., OKAMOTO, H., SUBRAMANIAN, P.R. & KACPRZAK, L. (1990): *Binary Alloy Phase Diagram* **2**. American Society for Metals, Metals Park, Ohio (1232-1233).

MISRA, K.C. & FLEET, M.E. (1973): Unit-cell parameters of monosulfide, pentlandite and taenite solid-solutions with the Fe–Ni–S system. *Mat. Res. Bull*. **8**, 669-678.

MORIMOTO, N. & KULLERUD, G. (1964): Pentlandite thermal expansion. *Carnegie Inst. Wash., Yearbook* **63**, 204-205.

PEREGOEDOVA, A & OHNENSTETTER, M. (2002): Collectors of Pt, Pd and Rh in a S-poor Fe–Ni–Cu sulfide system at 760°C: experimental data and application to ore deposits. *Can. Mineral*. **40**, 527-561.

RAGHAVAN, V. (1988): The Co–Fe–S (cobalt–iron–sulfur) system. *In* Phase Diagrams of Ternary Iron Alloys 2. Indian Institute of Metals, Calcutta, India (93-106).

RAJAMANI, V. & PREWITT, C.T. (1973): Crystal chemistry of natural pentlandites. *Can. Mineral*. **12**, 178-187.

_____ & _____ (1975a): Refinement of the structure of Co_9S_8. *Can. Mineral*. **13**, 75-78.

_____ & _____ (1975b): Thermal expansion of the pentlandite structure. *Am. Mineral.* **60**, 39-48.

RAU, H. (1976): Range of homogeneity and defect energetics in $Co_{1-x}S$. *J. Phys. Chem. Solids* **37**, 931-934.

ROSENQVIST, T. (1954): A thermodynamic study of the iron, cobalt and nickel sulfides. *J. Iron Steel Inst*. **176**, 37-57.

SHEWMAN, R.W. & CLARK, L.A. (1970): Pentlandite phase relations in the Fe–Ni–S system and notes on the monosulfide solid-solution. *Can. J. Earth Sci.* **7**, 419-426.

SINGLETON, M., NASH, P. & LEE, K.J. (1990): Ni–S. *In* Binary Alloy Phase Diagram **3** (T.B. Massalski, H. Okamoto, P.R. Subramanian & L. Kacprzak, eds.). American Society for Metals, Metals Park, Ohio (2850-2853).

SUGAKI, A. & KITAKAZE, A. (1992): Phase transition of pentlandite. *Proc. 29th Int. Geol. Congress* (*Kyoto*) **3**, 676 (abstr.).

_____ & _____ (1996): New data of high-pentlandite solid solution; study on the Fe–Ni–S system (5). *Joint Meeting Japan. Assoc. Mineral. Petrol. Econ. Geol., Mineral. Soc. Japan & Soc. Resource Geol.* (*Kanazawa*), 150 (abstr.).

_____ & _____ (1998): High form of pentlandite and its thermal stability. *Am. Mineral*. **83**, 133-140.

_____, _____ & HAYASHI, T. (1982): High-temperature phase of pentlandite. *Annual Meeting Mineral. Soc. Japan, Abstr.*, 22 (in Japanese).

_____, _____ & _____ (1983): New data on the pentlandite stability. *Mining Geol*. **33**, 63 (abstr., in Japanese).

_____, _____ & _____ (1984): The solid-solution of pentlandite and its phase relations at temperatures from 600° to 800°C. *J. Japan. Assoc. Mineral. Petrol. Econ. Geol*. **79**, 175-176 (abstr., in Japanese).

_____, SHIMA, H. & KITAKAZE, A. (1976): Application of Bence and Albee method to an analysis of sulfide minerals: Cu–Fe–Pb–Bi–S system. *J. Mineral. Soc. Japan* **12**, *Special Issue*, 85-92 (in Japanese).

SUMIYAMA, K., KADONO, M. & NAKAMURA, Y. (1983): Metastable *bcc* phase in sputtered Fe–Ni alloys. *Trans. Japan. Inst. Metals* **24**, 190-194.

SUTTON, A.L. & HUME-ROTHERY, W. (1955): The lattice spacings of solid-solutions of titanium, vanadium, chromium, manganese, cobalt and nickel in alpha-iron. *Philos. Mag*, **46**, 1295-1309.

VAASJOKI, O., HÄKLI, T.A. & TONTTI, M. (1974): The effect of cobalt on the thermal stability of pentlandite. *Econ. Geol*. **69**, 549-551.

Received January 15, 2003, revised manuscript February 20, 2004.